




# Hydrological, geochemical and land use drivers of greenhouse gas dynamics in eleven sub-tropical streams

Luke F. Andrews<sup>1</sup> · Praktan D. Wadnerkar<sup>1</sup> · Shane A. White<sup>1</sup> · Xiaogang Chen<sup>1,2</sup> · Rogger E. Correa<sup>1</sup> · Luke C. Jeffrey<sup>3</sup> · Isaac R. Santos<sup>1,4</sup> 

Received: 4 May 2020 / Accepted: 12 February 2021 / Published online: 14 March 2021  
© The Author(s) 2021

## Abstract

Greenhouse gas (GHG) emissions from freshwater streams are poorly quantified in sub-tropical climates, especially in the southern hemisphere where land use is rapidly changing. Here, we examined the distribution, potential drivers, and emissions of carbon dioxide (CO<sub>2</sub>), nitrous oxide (N<sub>2</sub>O) and methane (CH<sub>4</sub>) from eleven Australian freshwater streams with varying catchment land uses yet similar hydrology, geomorphology, and climate. These sub-tropical streams were a source of CO<sub>2</sub> ( $74 \pm 39$  mmol m<sup>-2</sup> day<sup>-1</sup>), CH<sub>4</sub> ( $0.04 \pm 0.06$  mmol m<sup>-2</sup> day<sup>-1</sup>), and N<sub>2</sub>O ( $4.01 \pm 5.98$  μmol m<sup>-2</sup> day<sup>-1</sup>) to the atmosphere. CO<sub>2</sub> accounted for ~97% of all CO<sub>2</sub>-equivalent emissions with CH<sub>4</sub> (~1.5%) and N<sub>2</sub>O (~1.5%) playing a minor role. Episodic rainfall events drove changes in stream GHG due to the release of soil NO<sub>x</sub> (nitrate + nitrite) and dissolved organic carbon (DOC). Groundwater discharge as traced by radon (<sup>222</sup>Rn, a natural groundwater tracer) was not an apparent source of CO<sub>2</sub> and CH<sub>4</sub>, but was a source of N<sub>2</sub>O in both agricultural and forest catchments. Land use played a subtle role on greenhouse gas dynamics. CO<sub>2</sub> and CH<sub>4</sub> increased with catchment forest cover during the wet period, while N<sub>2</sub>O and CH<sub>4</sub> increased with agricultural catchment area during the dry period. Overall, this study showed how DOC and NO<sub>x</sub>, land use, and rainfall events interact to drive spatial and temporal dynamics of GHG emissions in sub-tropical streams using multiple linear regression modelling. Increasing intensive agricultural land use will likely decrease regional CO<sub>2</sub> and CH<sub>4</sub> emissions, but increase N<sub>2</sub>O.

**Keywords** Climate change · Coastal carbon · Estuaries · Hydrology · Gas exchange · Water management

## Introduction

Freshwater systems have been recognised as an important source of greenhouse gases (GHGs), especially CO<sub>2</sub>, to the atmosphere (Cole et al. 2007; Drake et al. 2018; Li et al. 2018; Marx et al. 2017). Of the 5.1 Pg year<sup>-1</sup> of terrestrially derived carbon exported into continental waters, only 0.95 Pg year<sup>-1</sup> reaches the ocean (Drake et al. 2018). The lost carbon

is attributed to the outgassing of CO<sub>2</sub> (~97%) and CH<sub>4</sub> (~3%) (Drake et al. 2018; Marx et al. 2017; Sawakuchi et al. 2017). N<sub>2</sub>O is also considered an important contributor to GHG evasion from streams (Beaulieu et al. 2010), with microbial denitrification being the major source (Marzadri et al. 2017). Current flux estimates from global river systems vary from 0.68 Tg N–N<sub>2</sub>O year<sup>-1</sup> (Beaulieu et al. 2010) to 1.05 Tg N–N<sub>2</sub>O year<sup>-1</sup> (Seitzinger et al. 2010). While these absolute emission estimates for N<sub>2</sub>O are far lower than for stream CO<sub>2</sub> emissions (Drake et al. 2018), N<sub>2</sub>O has ~300 times the sustained warming potential (SWP) of CO<sub>2</sub> (Maavara et al. 2019). Direct measurements of aquatic greenhouse gases as well as spatiotemporal coverage remain limited (Cole et al. 2007).

At a local scale, the fluxes of GHGs are temporally and spatially driven by geochemical factors that are often related to the catchment landscape such as land use, climate, and hydrology (Atkins et al. 2017; Ni et al. 2020; Petrone 2010). The delivery of solutes such as dissolved organic matter (DOM), dissolved inorganic nitrogen (DIN), and aqueous forms of GHGs from the catchment landscape

✉ Isaac R. Santos  
isaac.santos@gu.se

<sup>1</sup> National Marine Science Centre, Southern Cross University, Coffs Harbour, Australia  
<sup>2</sup> Key Laboratory of Coastal Environment and Resources of Zhejiang Province, School of Engineering, Westlake University, Hangzhou 310024, China  
<sup>3</sup> SCU Geoscience, Southern Cross University, Lismore, Australia  
<sup>4</sup> Department of Marine Sciences, University of Gothenburg, Gothenburg, Sweden

into streams occurs during rainfall events or via groundwater discharge (Dinsmore et al. 2013; Marx et al. 2017). Rainfall events tend to alter stream pH, temperature, and dissolved oxygen (DO), which, in turn, affect the microbial production of GHGs in stream sediments as well as their solubility and fluxes at the air–water interface (Borges et al. 2015, 2018a; Webb et al. 2016). Furthermore, runoff events tend to increase surface water velocity and turbulence, enhancing GHG emissions (Hall and Ulseth 2020; Raymond et al. 2012). Aquifer recharge following rainfall drives the seepage of groundwater supersaturated in CO<sub>2</sub> (Sadat-Noori et al. 2015), CH<sub>4</sub> (Borges et al. 2018b), and N<sub>2</sub>O (Quick et al. 2019). In the absence of rainfall, streams tend to have longer water residence times which allow for internal aquatic processes (such as microbial respiration and photodegradation) and slow groundwater seepage to exert a stronger influence on GHG dynamics (Herreid et al. 2020; Marx et al. 2017; Smith and Kaushal 2015).

The effect of anthropogenic landscape modification on nutrient cycles within aquatic environments has been broadly investigated at local and global scales (Beusen et al. 2013; Canfield et al. 2010; Seitzinger et al. 2010; White et al. 2018). However, linkages between GHG dynamics and land use change have only begun to be explored (e.g., Herreid et al. 2020; Marx et al. 2017; Ni et al. 2019; Reading et al. 2020). Since pre-industrial times, carbon loading to inland waters has increased by as much as 1 Pg C year<sup>-1</sup> due to deforestation and agricultural intensification (Bass et al. 2014; Drake et al. 2018). Urbanisation also affects stream geochemical cycling through reduced hydrologic retention from impervious materials which may enhance loading of dissolved organic carbon (DOC) (Petroni 2010), nitrate (Petroni et al. 2008), and potentially modify GHG production pathways (Jeffrey et al. 2018b). Quantifying GHG fluxes from catchments which have undergone land use changes is crucial to understand mechanisms driving greenhouse gas emissions and predict future changes (Drake et al. 2018).

Aquatic GHG observations in tropical and sub-tropical latitudes, particularly in the Southern Hemisphere, are limited (Atkins et al. 2017; Drake et al. 2018; Musenze et al. 2014). In warmer tropical and sub-tropical systems, river discharge is often dominated by episodic rain events rather than more predictable seasonal cycles as seen in temperate climates (Looman et al. 2016b). Furthermore, most of the global CO<sub>2</sub> evasion from inland waters probably occurs at low latitudes, emphasising the need for increased spatial coverage of GHG investigations (Sawakuchi et al. 2017). This lack of spatial coverage also extends to upland streams which are under-represented given that they comprise up to 90% of terrestrial drainage patterns worldwide (Drake et al. 2018; MacDonald and Coe 2007). These streams are also important as they exhibit high surface area-to-volume ratios, which maximise the interface for GHG exchange with

the atmosphere and facilitate high levels of loading from the adjacent landscape through the hyporheic zone (Comer-Warner et al. 2019).

Here, we examined the concentrations, drivers, and potential fluxes of the three major GHGs (CO<sub>2</sub>, N<sub>2</sub>O, and CH<sub>4</sub>) from eleven sub-tropical freshwater streams with varying catchment land uses (forested, agricultural and mixed modified), yet similar hydrology, geomorphology, and climate. We use radon (<sup>222</sup>Rn, a natural groundwater tracer) to assess if stream GHGs are driven by surface runoff or groundwater discharge. We also quantify the relative contribution of the three main GHGs to total CO<sub>2</sub>-equivalents and Sustained Global Warming Potentials (SGWP; Neubauer and Megonigal 2015). Finally, we contrast our observations in sub-tropical Australia with more frequently investigated temperate river and creek systems.

## Materials and methods

### Study site

Sampling was conducted in 11 freshwater streams in northern New South Waters, Australia (Fig. 1), within a region characterised by humid sub-tropical climate (CfA according to the Köppen climate classification system) (BOM 2019). These freshwater catchments were selected based on their comparable geomorphology, climate, and hydrological characteristics, but contrasting land use (Fig. 1). Annual rainfall in the region is 1700 mm and ambient temperatures range from 10 to 28 °C. Most of the precipitation (about 65%) falls in the summer months between December and April (Wadnerkar et al. 2019 and references therein). Local precipitation drainage in the area is predominately mediated by small hydrologically responsive streams of low Strahler order due to the geographic confinements of the region. Vegetation in the upper and middle catchment areas is dominated by remnant wet-sclerophyll and mixed rainforest, whereas vegetation in the lower catchment is mainly restricted to the riparian zones composed of *Eucalyptus*, *Casuarina* and *Melaleuca* species (Looman et al. 2019). Soils are of basaltic origin, typically well drained with podzolic horizons (Milford 1999).

The study region has undergone significant landscape modification in the last century with widespread clearing of forests for urban, agricultural, and forestry development (Looman et al. 2019). Land was originally cleared for banana plantations on the hillslopes and grazing on the erosional valley fills (Conrad et al. 2017). Since the 1970s the banana industry has been superseded by other intensive horticultural practices such as blueberry (*Vaccinium* sp.) cultivation which have been linked to increased nitrogen and heavy metal loading in local streams and sediments (Conrad

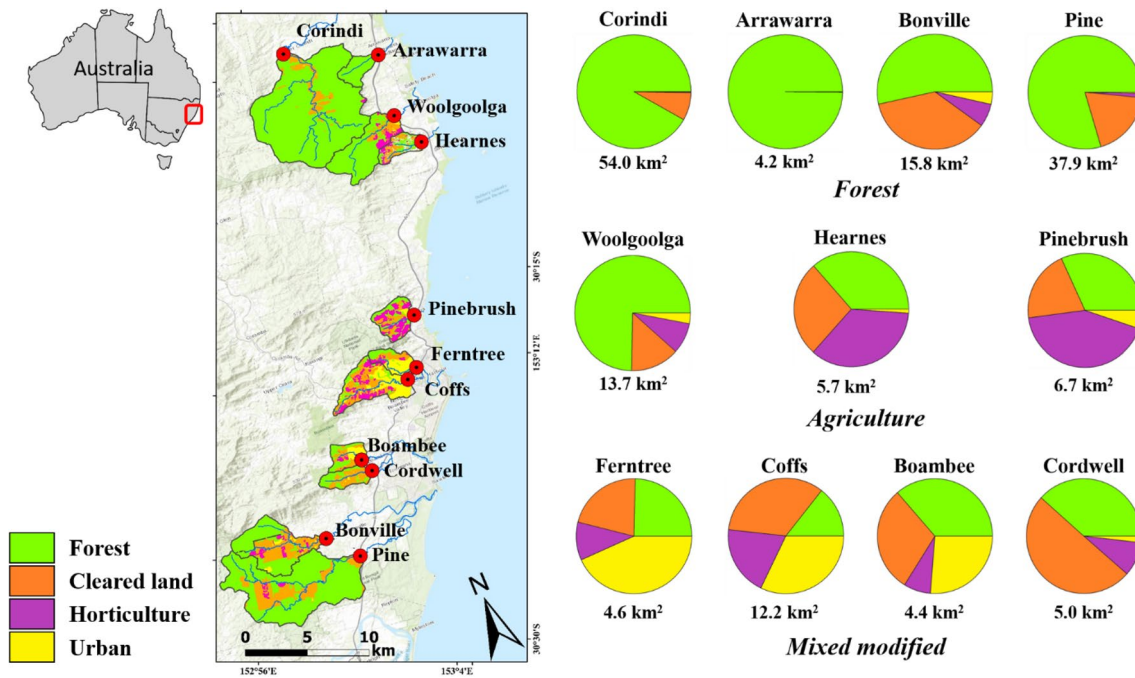


**Fig. 1** Map of study region with freshwater sub-catchment boundaries and sample sites indicated in red. Individual catchment land use classification on the right (north–south). See text for data source and analysis

et al. 2019, 2020; White et al. 2018). Population is concentrated around Coffs, Ferntree and Boambee catchments with population densities of  $\geq 18$  persons per  $\text{km}^2$  (Looman et al. 2019). These factors have led to the development of the current landscape which displays mosaic patterns of urban (residential, commercial, industrial), agricultural (grazing and horticulture including banana plantations, blueberry farms and hothouses), and forest (managed and natural) land uses (Fig. 1). Earlier observations of high nitrate in regional streams were linked to agricultural land use (Wadnerkar et al. 2021; White et al. 2018), while observations in four regional estuaries found greater DOC and  $\text{CO}_2$  in natural estuaries than modified systems (Looman et al. 2019). Here, we build on earlier regional work by focusing on freshwater sub-catchments at a broader spatial scale rather than focusing on the estuarine mixing gradient.

### Sampling and analysis

Creek water samples were collected at weekly intervals from 10 January to 2 May 2019, totalling 15 samples per site. Sampling locations within streams were selected based on the upper limit of the tidal reach (salinity  $< 2.0$ ) and hydrogeomorphology. During the first survey, four sites (Boambee, Cordwells, Bonville, and Woolgoolga) recorded salinity readings  $> 2.0$ , indicative of estuarine water penetration during extreme dry conditions. These outliers were removed from the dataset. DOC,  $\text{NO}_x$ , and GHGs ( $\text{CO}_2$ ,  $\text{CH}_4$ ,  $\text{N}_2\text{O}$ )

were sampled from surface stream water on each sampling occasion using a peristaltic pump. Ancillary parameters (temperature, salinity, pH, and DO) were measured in situ using a multimeter (HQ40d Hach, USA). While all the greenhouse gas data reported here are original, ancillary parameters including nutrient concentrations and stable isotopes in nitrate are reported in a companion paper (Wadnerkar et al. 2021).

DOC samples were collected using polyethylene syringes, filtered through pre-combusted  $0.7 \mu\text{m}$  GF/F filters (Whatman), and stored in 40 mL borosilicate vials (USP Type I) treated with  $30 \mu\text{L}$  of  $\text{H}_3\text{PO}_4$ . Vials were stored at  $3^\circ\text{C}$  for laboratory analysis. Total organic carbon (TOC) concentrations were assessed using an Aurora 1030 W TOC Analyser (Thermo Fisher Scientific, ConFLo IV).  $\text{NO}_x$  concentrations were determined colourimetrically on a Lachat Flow Injection Analyser (FIA). For that, water samples were collected in 10 mL polyethylene vials, filtered through a  $0.7 \mu\text{m}$  glass fibre syringe filter and frozen for laboratory analysis. GHGs samples were collected by extracting 50 mL of water in five polyethylene syringes and introducing gas with known partial pressures to create a water–air headspace gradient for gas transfer. The headspace was then injected into 1 L Tedlar gas (Supelco company) bags for analysis in a calibrated cavity ring down spectrometer (Picarro G2308) to determine  $\text{CO}_2$ ,  $\text{CH}_4$ , and  $\text{N}_2\text{O}$  values in air. The partial pressures, concentrations, and percent saturation of the GHGs in water were calculated from gas-specific solubility constants as a function

of salinity and temperature (Pierrot et al. 2009; Weiss and Price 1980; Yamamoto et al. 1976). Groundwater contributions to the streams were assessed using the naturally occurring radioactive isotope radon ( $^{222}\text{Rn}$ ; half-life = 3.8 days) (Burnett et al. 2001). Here, discrete samples were taken with 2 L HDPE plastic bottles which were sealed airtight until further analysis. Samples were run on a RAD7 (Durrige Company) in-air closed loop monitor, following methods outlined by Lee and Kim (2006). Radon is used as groundwater proxy enabling semi-quantitative temporal comparisons within a creek or spatial comparisons when the catchments have a similar geology (Atkins et al. 2016).

### Data interpretation and analysis

Upstream catchment boundaries and land use characteristics (Fig. 1) were identified using watershed delineation and data provided by the Coffs Harbour City Council Local Environment Plan (Parliamentary Counsel's Office 2013) on ArcGIS Spatial Analyst (Version 10.5.1, ESRI). The classification of land use was verified and adjusted using current satellite imagery from Google Earth and ground verification. Several of the catchments had cleared pastured landscapes which was categorised as 'cleared agricultural land'. Catchments were then categorised into forested, agricultural (cleared land + horticulture), and mixed modified (urban + agriculture) according to % coverage of each land use within the freshwater catchments (> 75% forest = forested, > 50% horticulture or cleared land = agricultural, < 50% agriculture and < 75% forest = mixed modified, Fig. 1). This method enabled a comparison of GHG observations to the degree and type of landscape modification. A preliminary attempt to have urban catchments (including Coffs and Ferntree creeks) as a separate category produced no additional insight or patterns, so we rely on three categories to simplify the analysis.

Rainfall and wind speed data were obtained from the Coffs Harbour Airport station (059151) (BOM 2019). Run-off was determined from the Australian Landscape Water Balance model (AWRA-L) (BOM 2019). Given only one rainfall station was available for hydrology comparisons, we assumed a homogenous parametrisation of daily runoff calculated from an average ( $\text{mm m}^{-2} \text{day}^{-1}$ ) of all catchments. To determine stream surface area for discharge calculations, creek cross-section profiles were recorded weekly at each creek making depth measurements every 50 cm across the stream. Stream cross-section area was then calculated using the trapezoidal rule ( $A = \frac{x_1+2x_2+x_3}{4} \times \text{width}$ ) with velocity being determined from AWRA-L runoff data (BOM 2019). The AWRA-L model gives an integrated water runoff measurement that represents the entire day and is comparable across catchments. GHG water-atmosphere fluxes ( $\text{mmol m}^{-2} \text{day}^{-1}$ ) were determined using:

$$\text{Flux} = k\alpha(C_w - C_{\text{atm}}) \quad (1)$$

where  $k$  is the gas transfer velocity ( $\text{m day}^{-1}$ ),  $\alpha$  is the solubility constants for each respective GHG,  $C_w$  the concentration of the gas in water, and  $C_{\text{atm}}$  is the ambient partial atmospheric pressure. Ambient atmospheric pressures used for  $\text{CO}_2$ ,  $\text{N}_2\text{O}$ , and  $\text{CH}_4$  were 412 ppm, 0.326 ppm, and 1.783 ppm, respectively, as observed from local air samples.

Gas transfer velocities were determined using two different empirical models to offer a range in possible emissions:

$$\text{Raymond and Cole (2001)} : k = 5.141u^{0.758}(\text{Sc}/660)^{-1/2} \quad (2)$$

$$\text{Borges et al. (2004)} : k = 1.91e^{0.35u}(\text{Sc}/600)^{-1/2} \quad (3)$$

Borges et al. (2004) where  $k$  is the transfer velocity ( $\text{cm h}^{-1}$ ),  $u$  is the wind speed at 10 m above ground ( $\text{m s}^{-1}$ ) obtained from BOM (2019),  $\text{Sc}$  is the Schmidt number of the gas at in situ temperature and salinity (Wanninkhof 1992). Given that the sampling sites were typically surrounded by riparian vegetation, influence from wind speed was likely to be minimal. Hence, the above gas transfer velocities were also calculated at  $0 \text{ km h}^{-1}$  wind speeds.

Net exports (potential emissions to the atmosphere assuming oversaturated values degas to the atmosphere in the downstream estuaries) were calculated by multiplying discharge with the difference between observed stream concentrations and concentrations at equilibrium with the atmosphere. This approach allows for an estimate of the potential emissions downstream of the observation site, assuming the aquatic GHGs will approach atmospheric equilibrium following degassing downstream.  $\text{CO}_2$  equivalent ( $\text{CO}_2\text{-eq}$ ) emissions were calculated using equations of solubility (Yamamoto et al. 1976), as well as 20 year sustained global warming potential (SGWP) estimations (Neubauer and Megonigal 2015) with  $\text{CO}_2\text{-eq}$  (20 year) =  $1\text{CO}_2 + 96\text{C H}_4 + 250\text{N}_2\text{O}$ . Pearson correlation coefficients from linear regressions between land use, GHGs, and physico-chemical drivers were calculated using IBM SPSS (25) (2-tailed, confidence interval: 0.05).

Multiple linear regression (MLR) models were also used to determine the most important water quality and landuse predictors of  $\text{CO}_2$ ,  $\text{CH}_4$ , and  $\text{N}_2\text{O}$  using Sigmaplot 13.0 (Systat Software, Inc). First, best subset linear regressions were performed to determine the ideal combinations of independent variables used in the models, with Mallows  $C_p$  value used as the best criterion. For the MLR models, constant variance testing was computed using the Spearman rank correlation between the absolute values of the residuals and the observed value of the dependent variables (Variance Inflation Factor flag values > 4.0 and Shapiro-Wilk normality testing set to  $p < 0.05$ ). The importance of the MLR model independent variables were determined by  $t$  values. MLR



models for each GHG was investigated for dry, wet and combined hydrological conditions. MLR models were also grouped into the dominant land usage type of each catchment then assessed for the best predictors of each GHG. The MLR model equations were then used to compare the modelled GHG's to the measured GHG's. As MLR models assume normal data distribution with constant variance, only the MLR models that passed Shapiro–Wilk normality testing were used in the interpretation.

## Results

### Hydrological conditions and ancillary parameters

Two contrasting hydrological regimes were observed across the 15-week sampling period: (1) a dry period with low rainfall (total of 86 mm in 63 days) and peak run off reaching  $0.25 \text{ mm m}^{-2} \text{ day}^{-1}$ , and (2) a wet period (total of 327 mm in 41 days) with spikes in catchment runoff of up to  $0.7 \text{ mm m}^{-2} \text{ day}^{-1}$  (Fig. 2). Rainfall for the whole sampling period (total of 413 mm) was below the historical average of 720 mm (BOM 2019). Streams during the dry period had low DO (18–65% saturation) and lower  $\text{NO}_x$  concentrations ( $0.4\text{--}10 \mu\text{mol L}^{-1}$ ) (Table 1, Fig. 3). In comparison, during the wet period streams experienced higher DO (25.4–85.5%)

**Fig. 2** Time series of daily rainfall and average catchment runoff (AWRA-L data, BOM 2019) over a 98-day sampling period in the Coffs Harbour region. Sampling days indicated by green triangles. Grey area denotes the wet period

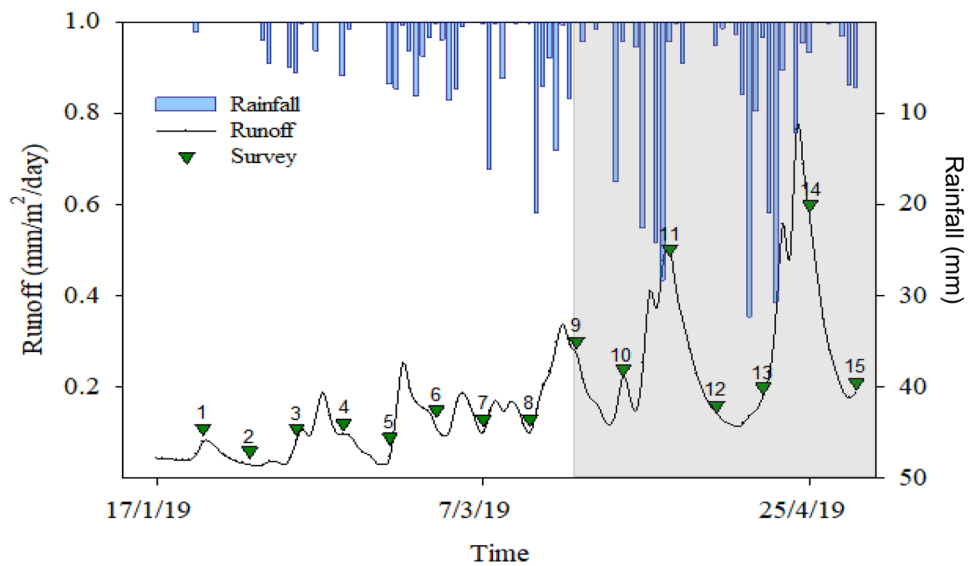
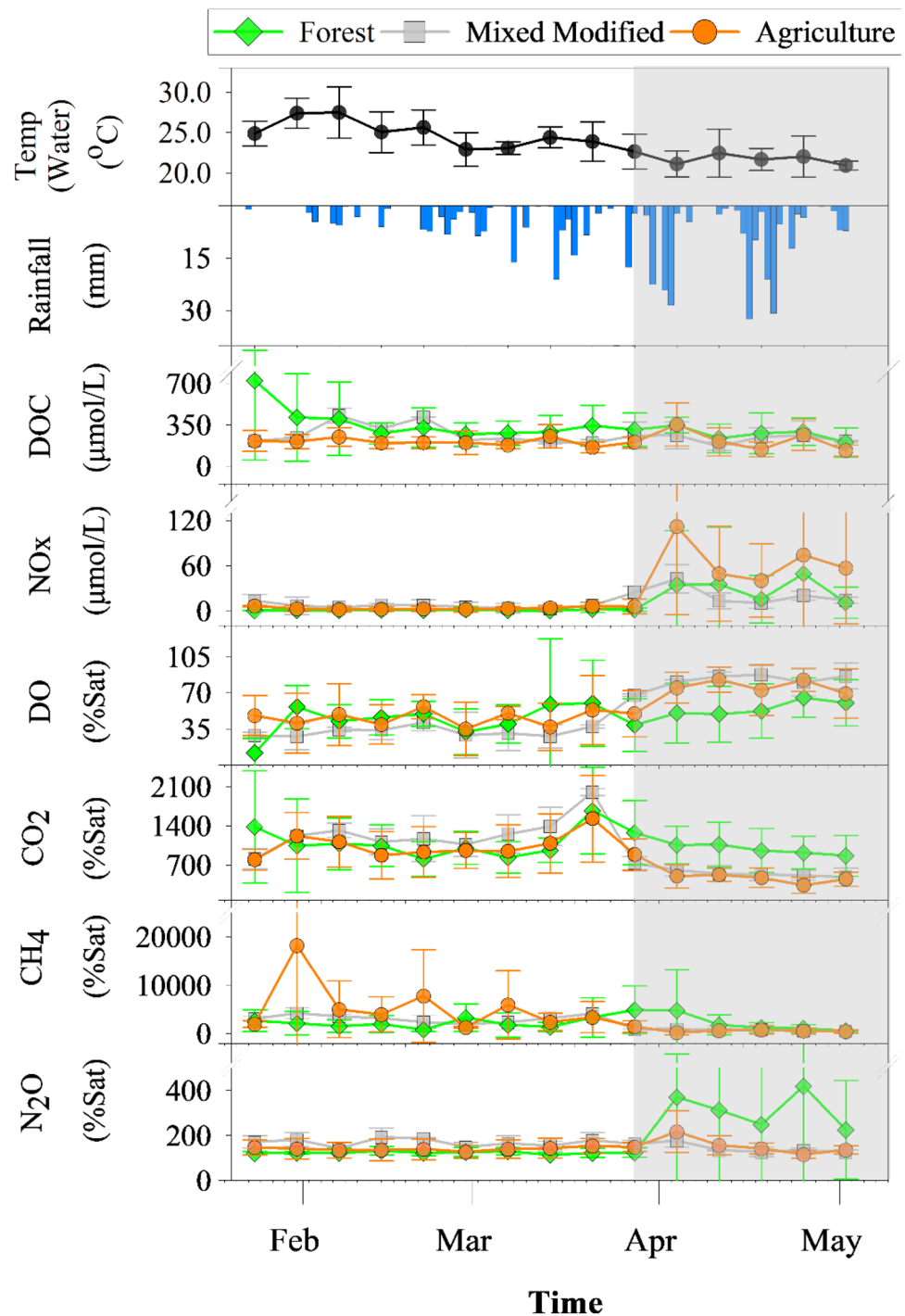


**Table 1** Mean ( $\pm$ SD) physico-chemical parameters recorded from each freshwater sub-catchment with reference to corresponding land use classification

| Creek        | Land use classification | Temp ( $^{\circ}\text{C}$ ) |                | pH            |               | DO (%)          |                 | Conductivity ( $\mu\text{Scm}^{-1}$ ) |               |
|--------------|-------------------------|-----------------------------|----------------|---------------|---------------|-----------------|-----------------|---------------------------------------|---------------|
|              |                         | Dry                         | Wet            | Dry           | Wet           | Dry             | Wet             | Dry                                   | Wet           |
| Corindi      | Forest                  | $26.5 \pm 2.3$              | $23.6 \pm 2.3$ | $6.9 \pm 0.1$ | $6.9 \pm 0.3$ | $55.6 \pm 48.5$ | $32.2 \pm 20.7$ | $150 \pm 61$                          | $152 \pm 8$   |
| Arrawarra    | Forest                  | $25.5 \pm 3.2$              | $23.5 \pm 2.3$ | $6.9 \pm 0.2$ | $7.2 \pm 0.4$ | $43.2 \pm 20.7$ | $52.8 \pm 12.7$ | $265 \pm 92$                          | $247 \pm 28$  |
| Woolgoolga   | Forest                  | $27.2 \pm 1.9$              | $23.4 \pm 2.2$ | $6.9 \pm 0.1$ | $7.0 \pm 0.3$ | $41.4 \pm 18.8$ | $69.2 \pm 26.5$ | $268 \pm 61$                          | $293 \pm 39$  |
| Hearnes Lake | Agriculture             | $25.4 \pm 1.8$              | $22.6 \pm 2.1$ | $7.0 \pm 0.2$ | $7.3 \pm 0.4$ | $44.8 \pm 14.9$ | $78.3 \pm 14.9$ | $329 \pm 220$                         | $391 \pm 131$ |
| Pinebrush    | Agriculture             | $25.9 \pm 3.2$              | $21.7 \pm 1.2$ | $6.8 \pm 0.1$ | $7.4 \pm 0.5$ | $65.8 \pm 10.6$ | $82.6 \pm 11.7$ | $195 \pm 96$                          | $296 \pm 177$ |
| Ferntree     | Mixed modified          | $25.5 \pm 2.2$              | $22.2 \pm 1.6$ | $6.9 \pm 0.0$ | $7.3 \pm 0.5$ | $31.7 \pm 13.4$ | $78.3 \pm 23.5$ | $183 \pm 78$                          | $166 \pm 30$  |
| Coffs        | Mixed modified          | $25.3 \pm 2.1$              | $22.0 \pm 0.9$ | $6.8 \pm 0.1$ | $7.2 \pm 0.4$ | $24.3 \pm 10.5$ | $70.4 \pm 17.4$ | $217 \pm 209$                         | $180 \pm 40$  |
| Boambee      | Mixed modified          | $23.4 \pm 1.1$              | $21.8 \pm 0.7$ | $6.6 \pm 0.0$ | $7.1 \pm 0.4$ | $39.7 \pm 7.9$  | $76.7 \pm 16.2$ | $167 \pm 7$                           | $168 \pm 45$  |
| Cordwells    | Agriculture             | $23.7 \pm 1.5$              | $21.1 \pm 0.5$ | $6.6 \pm 0.1$ | $7.0 \pm 0.4$ | $22.8 \pm 20.6$ | $47.3 \pm 27.1$ | $182 \pm 57$                          | $149 \pm 51$  |
| Bonville     | Mixed modified          | $23.3 \pm 1.2$              | $20.7 \pm 0.8$ | $6.6 \pm 0.0$ | $7.1 \pm 0.4$ | $62.2 \pm 2.6$  | $85.5 \pm 2.4$  | $88 \pm 19$                           | $70 \pm 3$    |
| Pine         | Forest                  | $24.0 \pm 1.4$              | $20.3 \pm 1.0$ | $6.3 \pm 0.1$ | $6.6 \pm 0.3$ | $18.4 \pm 7.4$  | $29.1 \pm 10.1$ | $97 \pm 77$                           | $167 \pm 237$ |

**Fig. 3** Time series of physico-chemical parameters and greenhouse gases recorded as means ( $n=4$  mixed modified,  $n=3$  agriculture,  $n=4$  forest) according to catchment classification. Shaded area indicates transition from dry to wet hydrology period



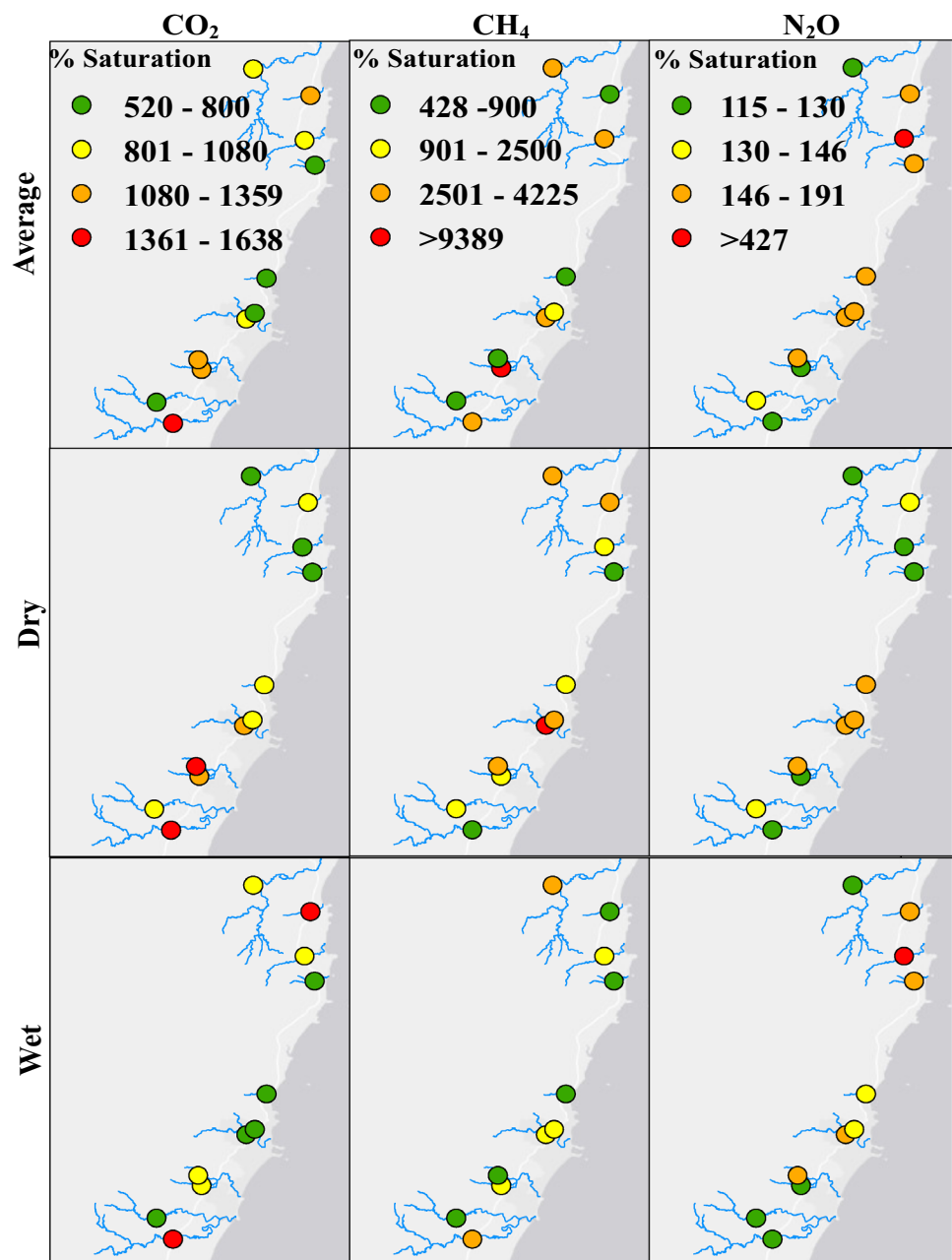
and  $\text{NO}_x$  ( $3\text{--}105 \mu\text{mol L}^{-1}$ ) with temperatures decreasing moving into autumn (Fig. 3; Supplementary Material). DOC concentrations exhibited no distinct trend throughout the sampling period ranging from  $250$  to  $450 \mu\text{mol L}^{-1}$  (Fig. 3).

### Greenhouse gases

$\text{CO}_2$  saturation ranged from  $520$  to  $1640\%$  (Fig. 4) peaking across most sites during the dry period before decreasing

during the wet period (with the exception of the forested catchments) (Fig. 3). The general decrease in  $\text{CO}_2$  moving into the wet period was substantiated by a significant inverse relationship with runoff ( $p < 0.01$ , Fig. 5). Positive correlations with radon were only apparent during the dry period (Fig. 6). Further,  $\text{CO}_2$  exhibited a significant negative correlation with DO (Fig. 7,  $p < 0.01$  Appendix A, Table 1) and a significant positive linear relationship with DOC in both hydrological periods (Fig. 7,  $p < 0.05$ , Table 2).

**Fig. 4** Mean greenhouse gas values (% sat) for each hydrological period



CH<sub>4</sub> saturation was highly variable between sites ranging from 428 to 9450% (Fig. 4). This variation was greatest during the dry period, with sites such as Cordwells (agricultural site) experiencing large spikes (>9400%) at surveys 2, 5, and 7 (Fig. 3). Overall, moving into the wet period CH<sub>4</sub> decreased, exhibiting a significant inverse relationship with runoff ( $p < 0.05$ , Fig. 5). In contrast to CO<sub>2</sub>, CH<sub>4</sub> displayed no correlations to radon across either the dry or wet period (Fig. 6). Further, as seen with CO<sub>2</sub>, CH<sub>4</sub> also negatively correlated with DO throughout the dry and wet periods (Fig. 7,  $p < 0.05$ , Table 2).

N<sub>2</sub>O saturation ranged from 115 to 190% saturation during the dry period and from 119 to 1430% during the

wet period (Fig. 3). The peak saturation observed at the Woolgoolga site was up to 10 times greater than other sites (Fig. 4, Supplementary Online Material). We suspect this is due to the site location immediately downstream of a hot-house facility and a short creek length for N<sub>2</sub>O to outgas. Transitioning into the wet period, N<sub>2</sub>O spiked at sample 11 across all catchments following consecutive days of > 20 mm rain (Fig. 3). In contrast to CO<sub>2</sub> and CH<sub>4</sub>, N<sub>2</sub>O significantly increased with increasing runoff ( $p < 0.01$ , Fig. 5) and in relation to <sup>222</sup>Rn (Fig. 6). Further, N<sub>2</sub>O exhibited a significant positive correlation with NO<sub>x</sub> concentrations across both hydrological regimes (Fig. 7,  $p < 0.01$ , Table 1) and with DOC during the wet period (Fig. 7,  $p < 0.05$ , Table 1).

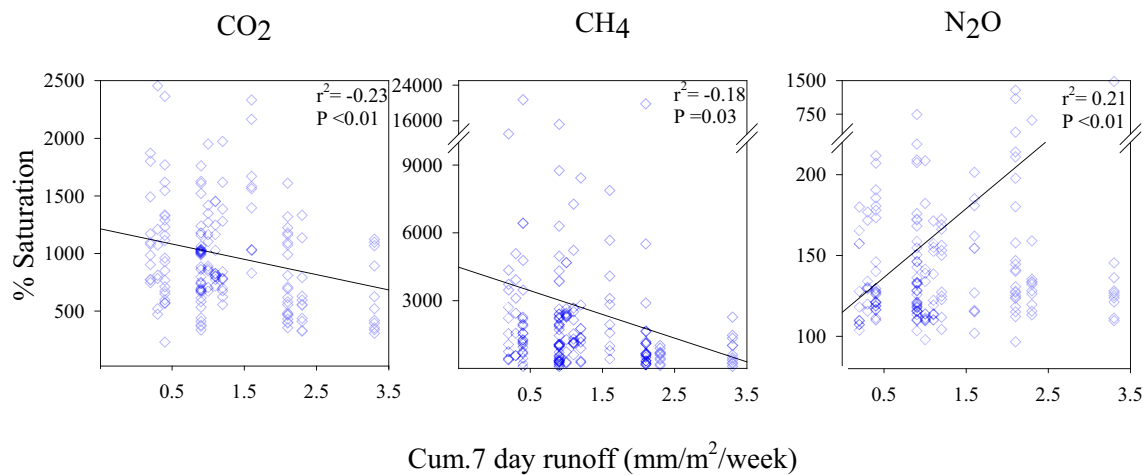


**Fig. 5** Scatter plot of mean GHG concentrations (% sat) versus 7 day cumulative runoff ( $\text{mm m}^{-2} \text{ day}$ ) obtained from AWRA-L data, BOM 2019. Lines indicate significance (Pearson's correlation 2-tailed,  $p=0.05$ )

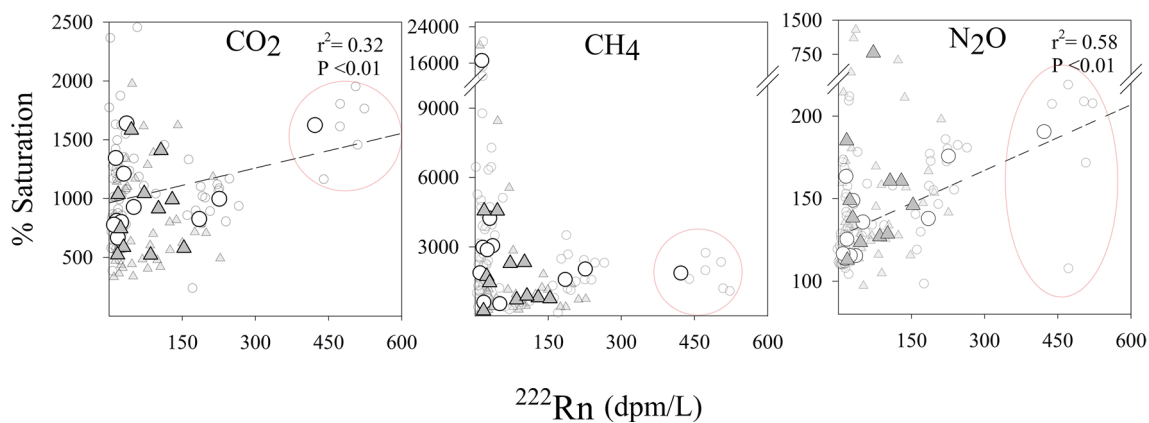


**Fig. 6** Scatter plot of GHGs versus  $^{222}\text{Rn}$ . Large symbols represent averages for each catchment, while smaller symbols show individual observations. Grey triangles represent wet conditions and white circles represent dry conditions. Dashed lines indicate significant correlations

relation during dry conditions only including outliers (red circles) (2-tailed Pearson,  $p=0.05$ ). Excluding the highlighted outliers results in different  $\text{CO}_2$  vs.  $^{222}\text{Rn}$  ( $p>0.05$ ,  $r^2=0.22$ ) and  $\text{N}_2\text{O}$  vs.  $^{222}\text{Rn}$  ( $p<0.05$ ,  $r^2=0.49$ ) regressions

## Hydrological and land use drivers of GHG fluxes

The hydrological period seemed to exert a major control on GHG distributions (Fig. 8). During the dry period, no correlations were found between catchment land use and  $\text{CO}_2$  (Fig. 8, Table 2). However, wet period  $\text{CO}_2$  saturations exhibited a significant positive correlation with forest area (% of catchment) ( $p<0.01$ , Table 2) and a negative correlation with increasing agriculture ( $p<0.01$ , Table 2) and mixed modified catchment area ( $p<0.01$ , Table 2). In contrast to  $\text{CO}_2$ ,  $\text{CH}_4$  increased significantly (Table 2) with agricultural catchment area across both hydrological regimes (Fig. 8). A positive correlation was also evident during the wet period with increasing forested ( $p<0.05$ ) and mixed modified ( $p=0.05$ ) catchment area (Fig. 8).

Whereas,  $\text{N}_2\text{O}$  showed a significant positive correlation with increasing agricultural and mixed modified catchment areas only during the dry period ( $p=0.043$ , Fig. 8).

Overall, streams were a source of all three GHGs to the atmosphere (Fig. 9). On average,  $\text{CO}_2$  fluxes in the present study were  $74 \pm 39 \text{ mol m}^{-2} \text{ day}^{-1}$  and accounted for 97% of SWGP for all streams (Fig. 9)  $\text{CH}_4$  fluxes were highly variable with an average of  $0.04 \pm 0.06 \text{ mmol m}^{-2} \text{ day}^{-1}$  (Fig. 9).  $\text{N}_2\text{O}$  displayed a net-positive flux at an average rate of  $4.01 \pm 5.98 \text{ } \mu\text{mol m}^{-2} \text{ day}^{-1}$  (Fig. 9). It is also worth noting that  $\text{CH}_4$  had a greater contribution to  $\text{CO}_2$  eq emissions during the dry (1.9% dry versus 1.1% wet), while  $\text{N}_2\text{O}$  had a greater contribution during the wet (2.0% wet versus 0.8% dry) (Fig. 9).



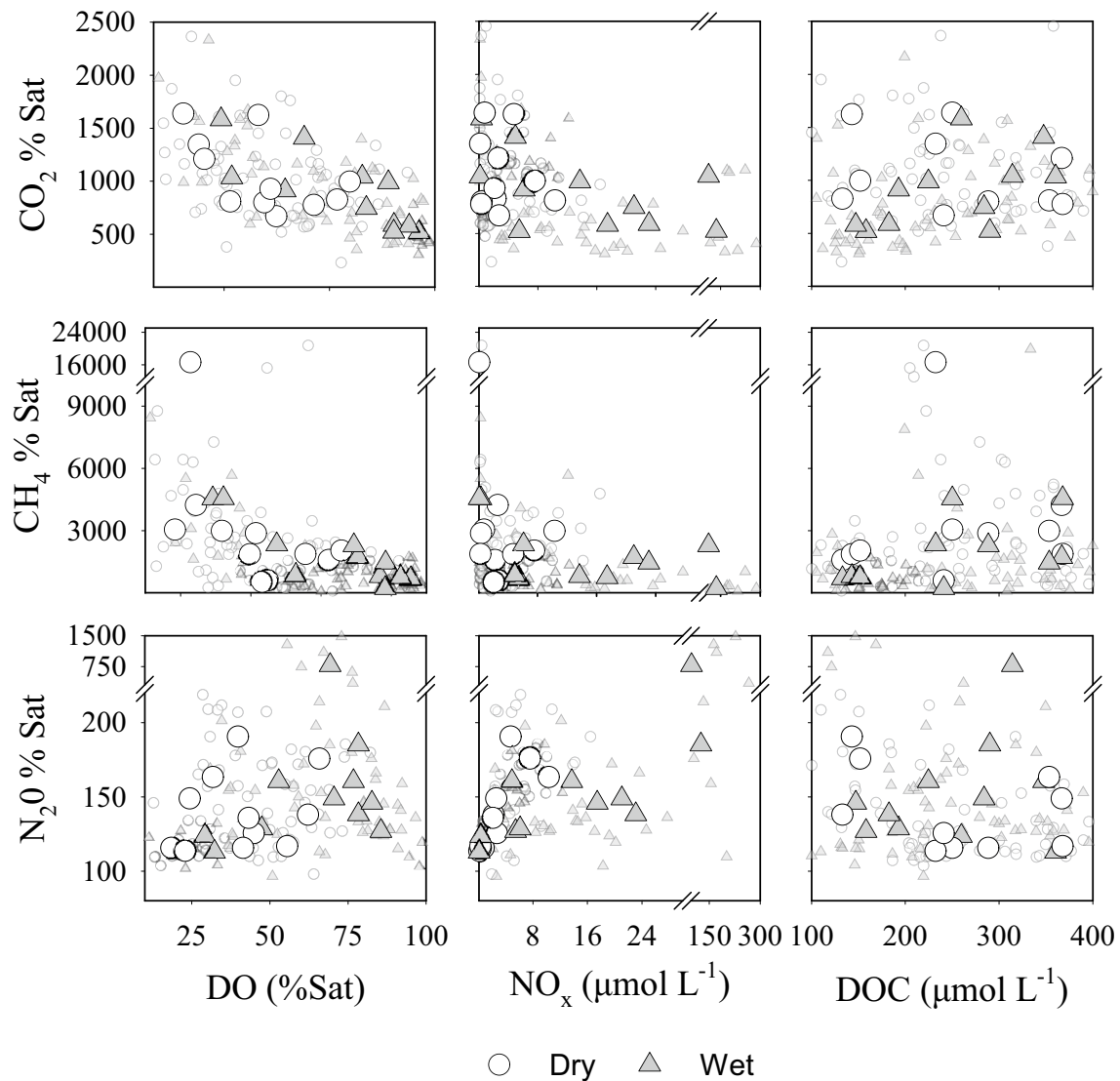


**Fig. 7** Scatter plot of mean (large symbols) GHG concentrations (% sat) versus ancillary measures (DO,  $\text{NO}_x$  and DOC). Smaller symbols show all data points, dry ( $n=84$ ) and wet ( $n=77$ ). For all  $r^2$  and  $p$  values see Table 2

### Multiple linear regression (MLR) models

Most GHG's could be modelled under differing land uses, however due to non-parametric data distribution, only  $\text{CO}_2$  was successfully modelled during the hydrological (wet) conditions (Shapiro–Wilk normality,  $p=0.94$ ) (Fig. 10). Generally,  $\text{CH}_4$  and  $\text{N}_2\text{O}$  were more difficult to model within hydrological grouped data due to low  $r^2$  values and non-parametric data distribution. Based off the MLR  $t$  values, positive  $^{222}\text{Rn}$  and negative pH and DO were important and significant predictors for  $\text{CO}_2$  during wet conditions (Fig. 10).  $\text{NO}_x$  and  $^{222}\text{Rn}$  were positive significant ( $p < 0.001$ ) predictors for  $\text{N}_2\text{O}$  in agricultural areas, whilst DO was the only negative significant ( $p < 0.001$ ) predictor for  $\text{CH}_4$  (Table 3).

When the data were grouped into dominant land use categories of each creek, all GHG's were again modelled (Fig. 11, Table 4). Most landuse MLR model passed normality tests except Agricultural  $\text{CH}_4$ , and the Forested  $\text{N}_2\text{O}$  and  $\text{CH}_4$  models (Fig. 11). Based off MLR  $t$ -values, positive significant  $^{222}\text{Rn}$ ,  $\text{NO}_x$  and DOC ( $p < 0.001$ ) were drivers of  $\text{N}_2\text{O}$  within Agricultural dominated creeks. For  $\text{CO}_2$ , both pH and DO were negative significant drivers ( $p < 0.001$ ) in Agricultural and Forest dominated creeks (Fig. 11, Table 4). Decreasing pH and DO were the main drivers of  $\text{CH}_4$  ( $p < 0.001$ ) in the Agricultural and Forest dominated creeks respectively (Table 4).

**Table 2** Pearson correlation matrix summary for % catchment land use (left) and DO, DOC, NO<sub>x</sub> (right) versus greenhouse gas concentrations during the dry (*n* = 84) and wet (*n* = 77) periods

| Hydrology period | Catchment land use |                       | CO <sub>2</sub>  | CH <sub>4</sub> | N <sub>2</sub> O | Physico-chemical parameters |                       | CO <sub>2</sub>  | CH <sub>4</sub>  | N <sub>2</sub> O |
|------------------|--------------------|-----------------------|------------------|-----------------|------------------|-----------------------------|-----------------------|------------------|------------------|------------------|
| Dry              | Agriculture        | <i>r</i> <sup>2</sup> | 0.023            | 0.23            | 0.22             | DO                          | <i>r</i> <sup>2</sup> | 0.31             | 0.27             | 0.15             |
|                  |                    | <i>p</i> value        | 0.83             | <b>0.03</b>     | <b>0.04</b>      |                             | <i>p</i> value        | <b>&lt; 0.01</b> | <b>0.01</b>      | 0.16             |
|                  | Forest             | <i>r</i> <sup>2</sup> | -0.08            | -0.16           | -0.46            | NO <sub>x</sub>             | <i>r</i> <sup>2</sup> | -0.11            | -0.14            | 0.70             |
|                  |                    | <i>p</i> value        | 0.44             | 0.13            | <b>&lt; 0.01</b> |                             | <i>p</i> value        | 0.28             | 0.19             | <b>&lt; 0.01</b> |
|                  | Mixed Modified     | <i>r</i> <sup>2</sup> | 0.08             | 0.16            | 0.46             | DOC                         | <i>r</i> <sup>2</sup> | -0.23            | -0.0             | -0.16            |
|                  |                    | <i>p</i> value        | 0.44             | 0.13            | 0.13             |                             | <i>p</i> value        | <b>0.03</b>      | 0.39             | 0.13             |
| Wet              | Agriculture        | <i>r</i> <sup>2</sup> | -0.45            | -0.20           | -0.07            | DO                          | <i>r</i> <sup>2</sup> | -0.70            | -0.60            | 0.04             |
|                  |                    | <i>p</i> value        | <b>&lt; 0.01</b> | 0.05            | 0.49             |                             | <i>p</i> value        | <b>&lt; 0.01</b> | <b>&lt; 0.01</b> | 0.73             |
|                  | Forest             | <i>r</i> <sup>2</sup> | 0.46             | 0.23            | 0.18             | NO <sub>x</sub>             | <i>r</i> <sup>2</sup> | -0.22            | -0.215           | 0.65             |
|                  |                    | <i>p</i> value        | <b>&lt; 0.01</b> | <b>0.04</b>     | 0.10             |                             | <i>p</i> value        | 0.05             | 0.05             | <b>&lt; 0.01</b> |
|                  | Mixed modified     | <i>r</i> <sup>2</sup> | -0.46            | -0.23           | -0.18            | DOC                         | <i>r</i> <sup>2</sup> | 0.26             | 0.20             | 0.24             |
|                  |                    | <i>p</i> value        | <b>&lt; 0.01</b> | <b>0.04</b>     | 0.10             |                             | <i>p</i> value        | <b>0.02</b>      | 0.08             | <b>0.03</b>      |

Values in bold denote significance at the 0.05 level (two-tailed)

## Discussion

Assessing the drivers of GHGs within streams is crucial for developing carbon and nitrogen budgets and predictive models in rapidly changing catchments (Drake et al. 2018). Insights into our hypotheses that land use drives GHGs in streams were obtained by establishing links between geochemical proxies (DOC, NO<sub>x</sub>, and DO) and GHGs within streams (Atkins et al. 2017; Seitzinger and Kroeze 1998; Stanley et al. 2016). Hydrological period and land use effected geochemical pathways, nutrient concentrations and physical processes to influence GHGs in streams (Figs. 10 and 11). Groundwater discharge was a not a major source of CO<sub>2</sub> and CH<sub>4</sub>, but seemed to release N<sub>2</sub>O from soils. In contrast to earlier work in temperate streams (Butman and Raymond 2011; Hutchins et al. 2019), land use had only a minor, subtle effect on greenhouse gas spatial variations in these sub-tropical streams. Here, we discuss the hydrological, geochemical, and land use drivers of GHG emissions and compare our results from sub-tropical streams to the literature on tropical and temperate streams.

### Hydrological and geochemical drivers of GHG dynamics

Overall, CH<sub>4</sub> and CO<sub>2</sub> showed higher saturations during the dry than the wet period. Higher CO<sub>2</sub> and CH<sub>4</sub> during low flow (dry) conditions is common across various fluvial settings (Hope et al. 2001). Physical controls over GHG transfer velocities are also likely to play an important role in driving this relationship (Raymond et al. 2012). Low flow conditions increase water residence times, therefore reducing stream turbulence limiting gaseous emissions to the atmosphere and

promoting the accumulation of GHGs within streams (Jeffrey et al. 2018a; Rocher-Ros et al. 2019; Webb et al. 2016). This concept is substantiated by CO<sub>2</sub> and CH<sub>4</sub> increases during low DO saturations during the dry period (Table 3), implying instream respiration and subsequent accumulation of CO<sub>2</sub> and CH<sub>4</sub> in surface waters (Atkins et al. 2017; Borges et al. 2019; Macklin et al. 2014).

Increased turbulence and flow contributed to the observed decrease in surface water CO<sub>2</sub> and CH<sub>4</sub> saturations during the wet period (Borges et al. 2018b; Rocher-Ros et al. 2019). During the wet conditions, groundwater inputs of low DO water may explain the positive relationship between <sup>222</sup>Rn and CO<sub>2</sub> saturation (as supported by the MLR in Fig. 10). Overall, DO and flow regime seem to play a crucial role driving the temporal variability of CH<sub>4</sub> in sub-tropical streams similar to Northern Hemisphere streams. We also found a negative relationship between DOC and CO<sub>2</sub> during the dry period and a positive relationship during the wet period. The negative correlation during dry conditions supports our interpretation of instream metabolism dominating the CO<sub>2</sub> production pathway during low flow conditions (Marx et al. 2017). However, the positive relationship between DOC and CO<sub>2</sub> during the wet period suggests an alternate mechanism driving the relationship and might be due to a common source delivery from the soil landscape during runoff events (Hotchkiss et al. 2015) and/or groundwater inputs as traced by <sup>222</sup>Rn (Fig. 10, Table 3). After extended dry periods, flushing events tend to remove accumulated DOC and CO<sub>2</sub> from the soils into streams (Bodmer et al. 2016).

In contrast to CO<sub>2</sub> and CH<sub>4</sub>, N<sub>2</sub>O significantly increased with runoff and remained relatively constant throughout the dry period. This is likely explained by a combination

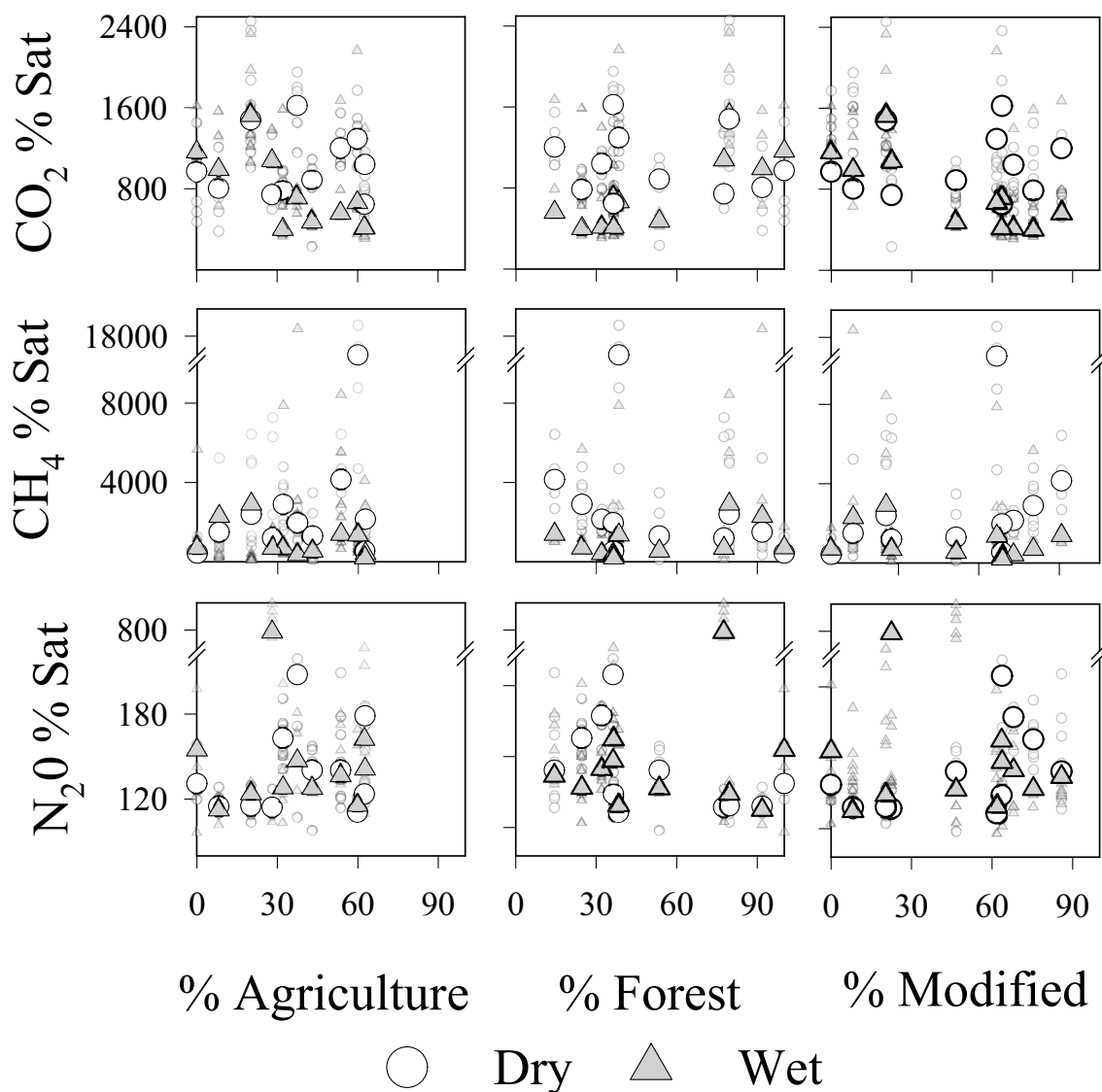


**Fig. 8** Scatter plot of median (large symbols) GHG concentrations (% sat) versus % land use according to catchment area. Smaller symbols show all data points. Dashed lines indicate significance (Pearson's

correlation 2-tailed,  $p=0.05$ ) during the dry ( $n=84$ ) and solid lines during the wet ( $n=77$ ) For all  $r^2$  and  $p$  values see Table 2

of (1) direct loading from soils whereby NO<sub>x</sub> and N<sub>2</sub>O enter streams simultaneously (Wilcock and Sorrell 2007), or (2) indirectly through increased availability of DIN facilitating instream N<sub>2</sub>O production (Quick et al. 2019). Given the simultaneous occurrence of high CH<sub>4</sub> from low oxygen sediments during the dry period and unlikely suspension of sediment particles due to longer water residence, it is likely that benthic denitrification processes are driving the production of N<sub>2</sub>O during the dry period. The source of DIN during dry conditions may be either shallow groundwater or in-stream organic nitrogen (Seitzinger and Kroeze 1998) as supported by the positive relationship of both <sup>222</sup>Rn and NO<sub>x</sub> with N<sub>2</sub>O in the dry period MLR (Fig. 10, Table 3). Groundwater discharge is commonly

neglected in riverine GHGs assessments (Atkins et al. 2017; Drake et al. 2018). During the wet period, the only significant correlation between radon and GHG's was with CO<sub>2</sub> (Fig. 10), which was probably due to increased surface water connectivity with soils following rain events (Atkins et al. 2013; Looman et al. 2016a) or the natural geomorphological settings of the catchments that favours surface runoff over groundwater flow (Reid and Iverson 1992). In contrast, N<sub>2</sub>O (when outliers were removed) displayed positive relationships with radon during the dry period, suggesting that groundwater plays a role in N<sub>2</sub>O dynamics either directly (i.e., delivering subsurface waters elevated in N<sub>2</sub>O), or indirectly (i.e., delivering DIN that fuels N<sub>2</sub>O production within the stream).

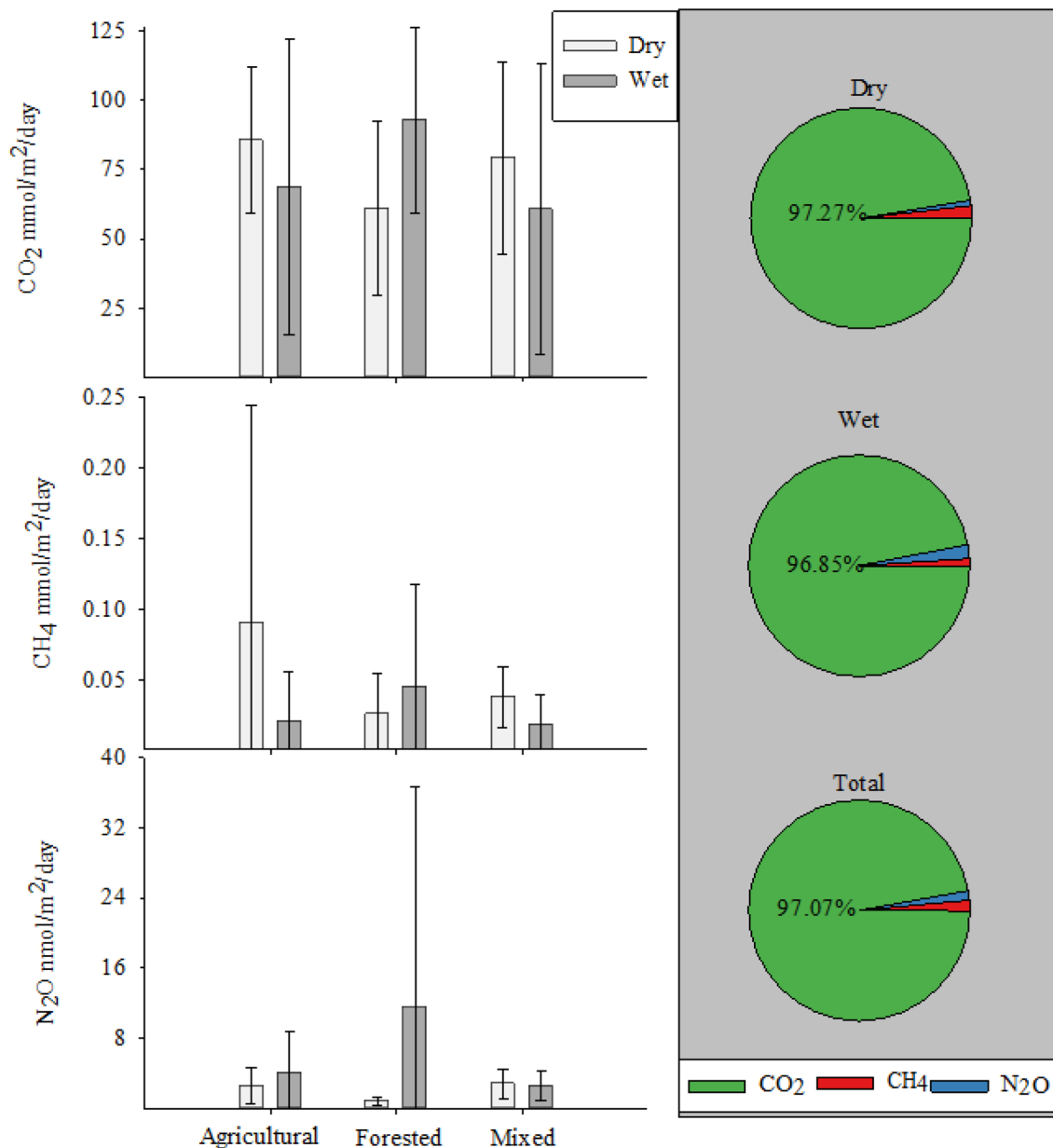


**Fig. 9** Mean ( $\pm$ SD) fluxes of GHGs from each catchment classification in relation to the hydrology period (left). (Right) The average % contribution of each GHG in relation to total SWGP (20 years) CO<sub>2</sub>-equivalence emissions (Neubauer and Megonigal 2015) across all streams

### Influence of land use on GHG dynamics

The influence of land use on aquatic greenhouse gases can be complex and variable, and could not be clearly observed in this investigation. In a preliminary analysis, we found no distinct patterns in the two catchments with significant urban development (Coffs and Ferntree, see Fig. 1). Hence, these urban catchments were included in the modified group. CO<sub>2</sub> increased with forest cover and decreased with mixed modified and agricultural land cover, as previously observed in estuaries in the same area (Looman et al. 2019). The

transport of dissolved nitrogen from modified catchments to the creek during the wet period can stimulate primary productivity and CO<sub>2</sub> consumption (Borges and Gypens 2010). Similar to our observations, riverine CO<sub>2</sub> levels were positively influenced by forested biomes in boreal streams (Hutchins et al. 2019). Forest soils often have higher rates of soil respiration and OM degradation than agricultural soils (Butman and Raymond 2011). These processes are enhanced at sub-tropical and tropical latitudes due to higher temperatures as well as greater terrestrial primary productivity (Butman and Raymond 2011). Other studies found higher CO<sub>2</sub>



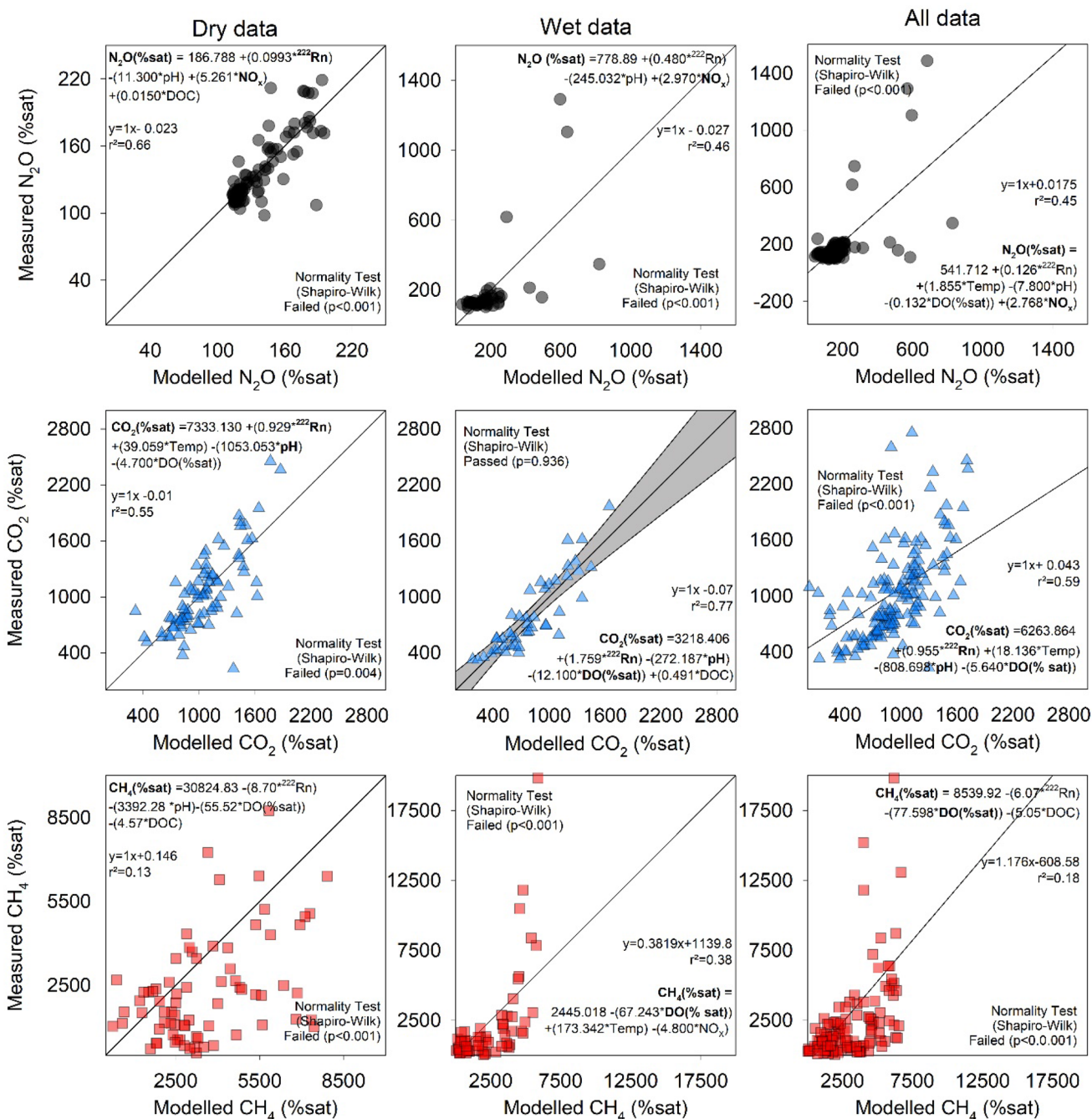


**Fig. 10** Measured GHG's vs MLR modelled GHG's used to predict the most important drivers under various hydrological conditions of the study. Different axis scales, most significant drivers ( $p < 0.001$ )

are highlighted in bold within each equation, solid lines represent the linear regression, shaded areas are 99% confidence intervals only shown where parametric data passed Shapiro–Wilk normality tests

fluxes within forested catchments during the wet period (Bodmer et al. 2016; Borges et al. 2018a), most likely related to higher DOC exports into nearby waterways (Atkins et al. 2017; Burgos et al. 2015). No relationships were evident between CO<sub>2</sub> and land use during the dry period, possibly as a result of reduced connectivity to the upstream landscape

allowing instream processes to mask catchment influences on CO<sub>2</sub> (Webb et al. 2019).

Assessing the influence of land use on CH<sub>4</sub> is challenging, given its variability shown across streams and rivers globally (Stanley et al. 2016). In sub-tropical Australia, CH<sub>4</sub> was positively related with agriculture cover during the dry period. While there is limited direct links between stream

**Table 3** Summary of *t* values generated from the MLR models showing most important predictors of N<sub>2</sub>O, CO<sub>2</sub> and CH<sub>4</sub> under differing hydrological regimes

| Drivers                        | All hydrological data |                 |                 | Dry hydrological data |                 |                 | Wet hydrological data |                 |                 |
|--------------------------------|-----------------------|-----------------|-----------------|-----------------------|-----------------|-----------------|-----------------------|-----------------|-----------------|
|                                | N <sub>2</sub> O      | CO <sub>2</sub> | CH <sub>4</sub> | N <sub>2</sub> O      | CO <sub>2</sub> | CH <sub>4</sub> | N <sub>2</sub> O      | CO <sub>2</sub> | CH <sub>4</sub> |
| <sup>222</sup> Rn              | 1.40                  | <b>4.13</b>     | -1.40           | <b>5.87</b>           | <b>3.51</b>     | -1.55           | 1.04                  | <b>3.37</b>     | -               |
| Temp                           | 0.40                  | 1.90            | -               |                       | <b>2.56</b>     | -               | -                     | -               | 0.46            |
| pH                             | -1.47                 | <b>-6.88</b>    | -               | -1.24                 | <b>-7.05</b>    | -1.06           | -2.02                 | -1.68           | 0.37            |
| DO (%sat)                      | -0.30                 | <b>-5.03</b>    | <b>-4.35</b>    | -                     | <b>-3.12</b>    | -2.39           | -                     | <b>-7.16</b>    | <b>-3.43</b>    |
| NO <sub>x</sub>                | <b>9.60</b>           | -               | -               | <b>8.45</b>           | -               | -               | <b>5.77</b>           | -               | -0.76           |
| DOC                            | -                     | -               | -1.85           | 1.37                  | -               | -1.23           | -                     | 1.70            | -               |
| <i>n</i>                       | 127                   | 127             | 127             | 83                    | 83              | 83              | 44                    | 44              | 44              |
| Adjusted <i>r</i> <sup>2</sup> | 0.43                  | 0.58            | 0.14            | 0.65                  | 0.53            | 0.08            | 0.42                  | 0.75            | 0.75            |
| Model                          | 5                     | 5               | 3               | 4                     | 4               | 4               | 3                     | 4               | 4               |

Significant drivers of GHG's where  $p < 0.001$  are in bold, and where  $p < 0.05$  are in bold italic font

CH<sub>4</sub> and agriculture cover (Stanley et al. 2016), previous studies have also found elevated CH<sub>4</sub> associated with agricultural catchments (Borges et al. 2018a) or the proportion of wetlands within a catchment (Herreid et al. 2020). The accumulation of fine sediments in agricultural catchments can cause streambeds to become prone to anoxic conditions, favourable to methanogenesis (Stanley et al. 2016). Here, we demonstrated that the relationship between elevated CH<sub>4</sub> production and agricultural land deteriorated following rainfall events. This is likely due to shorter water residence time, enhanced oxygenation and dilution preventing the accumulation of CH<sub>4</sub> from sediment methanogenesis (Stanley et al. 2016).

Interestingly, moving into the wet period, CH<sub>4</sub> increased with increasing forest cover, which is similar to observations from the Northern Hemisphere (Stanley et al. 2016). Shallow flow paths through the riparian zone which adjoins forest soils rich in OM has contributed to stream CH<sub>4</sub> concentrations in the US (Jones and Mulholland 1998). In subtropical Australia, while land use may act as an important driver of CH<sub>4</sub> production, episodic rainfall seems to explain most of CH<sub>4</sub> dynamics. As opposed to streams in the Northern Hemisphere which are driven by snowmelt and seasonal falls (Borges et al. 2018a; Crawford et al. 2017), hydrology in Australia is driven mostly by episodic rain events that beak prolonged drought periods.

Spatial variations in N<sub>2</sub>O during the dry period were strongly associated with increasing agricultural and mixed modified land cover. Similar to our observations, significantly lower N<sub>2</sub>O concentrations were found with increasing forest cover in the tropical Congo (Borges et al. 2019) and Guadalete rivers (Burgos et al. 2015) due to limited application of fertilisers and delivery of DIN from agricultural landscapes. Forested catchments have far lower NO<sub>x</sub> concentrations in comparison to other catchments. NO<sub>x</sub> availability is an important driver of N<sub>2</sub>O in streams in the Northern

(Audet et al. 2017; Borges et al. 2018a) and Southern Hemisphere (Mwanake et al. 2019; Wilcock and Sorrell 2007) and was a significant driver of N<sub>2</sub>O in the agricultural MLR model (Fig. 11, Table 4). A positive relationship between land use and NO<sub>x</sub> has also been found in the region (Reading et al. 2020; Wadnerkar et al. 2021; White et al. 2018) as well as several other agricultural streams (Audet et al. 2017; Wilcock and Sorrell 2007). Interestingly, during the wet period, high NO<sub>x</sub> concentrations within the agricultural catchments did related to increased N<sub>2</sub>O (Fig. 7). This may be related to reduced groundwater influence during rain events (White et al. 2018) in combination with higher dissolved oxygen saturation, which might have compromised denitrification-related N<sub>2</sub>O production within the modified and agricultural streams. Alternatively, given that our agricultural sites had relatively lower levels of DOC and high NO<sub>x</sub>, conversion of NO<sub>x</sub> to N<sub>2</sub>O within these sites could have potentially been compromised by carbon limitation (Rosamond et al. 2012; Schade et al. 2016). DOC:NO<sub>3</sub><sup>-</sup> ratios are an indicator of microbial metabolism and carbon availability, explaining much of the distribution of N<sub>2</sub>O in urban streams in Baltimore (USA) receiving multiple anthropogenic inputs (Smith et al. 2017). However, no relationships were observed between DOC:NO<sub>3</sub><sup>-</sup> ratios and N<sub>2</sub>O within individual creeks, or when combining all systems, implying DOC availability is not limiting N<sub>2</sub>O production.

DIN is transported into streams primarily by surface runoff during rainfall events with a minor contribution of groundwater discharge in this region (Wadnerkar et al. 2019; White et al. 2018). Given the significant MLR relationships, and linear correlation between N<sub>2</sub>O and radon during the dry period, groundwater discharge may be supplying some N<sub>2</sub>O to streams within our modified and agricultural catchments as observed in the Congo River (Borges et al. 2019). This process may be driven by the common practice of fertigation in the region (Kaine and Giddings 2016), which can facilitate

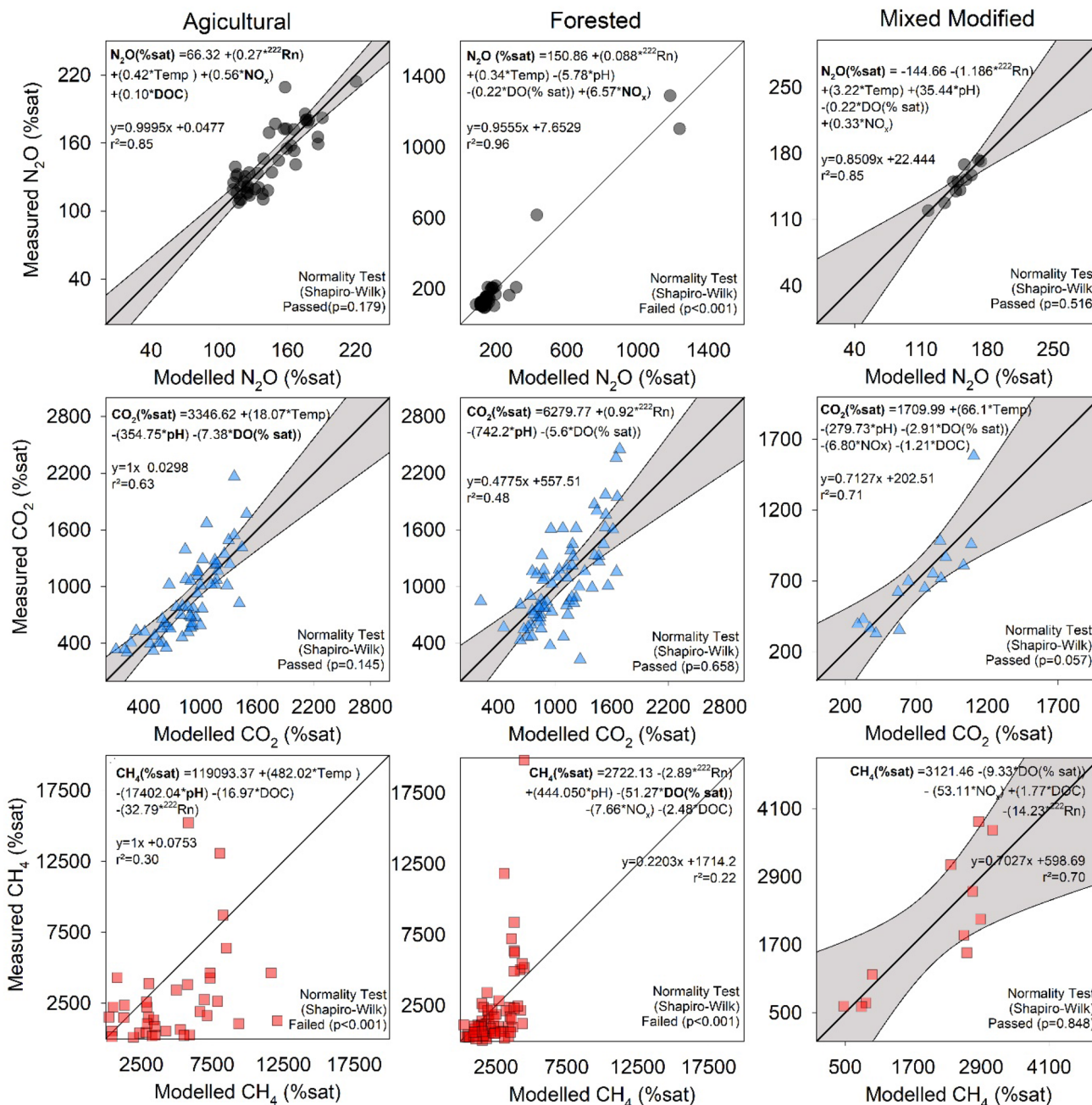


**Fig. 11** Measured GHG's vs MLR modelled GHG's used to predict the most important drivers under dominant land use types of the study. Different axis scales, most significant drivers ( $p < 0.001$ ) are

highlighted in bold within each equation, solid lines represent the linear regression, shaded areas are 99% confidence intervals only shown where parametric data passed Shapiro–Wilk normality tests

groundwater flows rich in nitrogen into streams during dry conditions, potentially contributing to N<sub>2</sub>O accumulation. Furthermore, hydrological modification through vegetation clearing for agriculture can enhance overland flow and groundwater recharge, creating more hydrologically responsive streams (Looman et al. 2019; Petrone 2010). This means that lower rainfall totals are required to move nitrate and

GHGs through the soil horizon, contributing to the higher N<sub>2</sub>O fluxes and concentrations seen during the drier period.

### CO<sub>2</sub>, CH<sub>4</sub>, and N<sub>2</sub>O air–water fluxes comparison

Streams in sub-tropical Australia acted as sources of greenhouse gases, generating net positive air–water fluxes to the atmosphere. On average, CO<sub>2</sub> fluxes across all catchments



**Table 4** Summary of *t* values generated from the MLR models showing most important predictors of N<sub>2</sub>O, CO<sub>2</sub> and CH<sub>4</sub> across different land uses

| Drivers                        | Agricultural catchments |                 |                 | Forest catchments |                 |                 | Mixed modified catchments |                 |                 |
|--------------------------------|-------------------------|-----------------|-----------------|-------------------|-----------------|-----------------|---------------------------|-----------------|-----------------|
|                                | N <sub>2</sub> O        | CO <sub>2</sub> | CH <sub>4</sub> | N <sub>2</sub> O  | CO <sub>2</sub> | CH <sub>4</sub> | N <sub>2</sub> O          | CO <sub>2</sub> | CH <sub>4</sub> |
| <sup>222</sup> Rn              | <b>8.07</b>             | –               | – <b>2.25</b>   | <b>2.25</b>       | <b>2.89</b>     | –1.07           | –2.01                     | –               | –0.41           |
| Temp                           | 0.42                    | <b>3.15</b>     | 1.16            | 0.17              | –               | –               | –1.99                     | 1.07            | –               |
| pH                             | –                       | – <b>5.93</b>   | – <b>3.46</b>   | –0.27             | – <b>4.20</b>   | 0.28            | 1.02                      | –0.26           | –               |
| DO (%sat)                      | –                       | – <b>3.49</b>   | –               | –1.06             | – <b>3.39</b>   | – <b>3.47</b>   | –1.20                     | –1.90           | –0.57           |
| NO <sub>x</sub>                | <b>9.58</b>             | –               | –               | <b>35.8</b>       | –               | –0.63           | 0.69                      | –0.42           | –1.34           |
| DOC                            | <b>6.26</b>             | –               | –1.58           | –                 | –               | –1.34           | –                         | –0.26           | 0.70            |
| <i>n</i>                       | 47                      | 47              | 47              | 87                | 87              | 87              | 11                        | 11              | 11              |
| Adjusted <i>r</i> <sup>2</sup> | 0.85                    | 0.77            | 0.30            | 0.96              | 0.48            | 0.22            | 0.85                      | 0.84            | 0.70            |
| Model                          | 4                       | 3               | 4               | 5                 | 3               | 5               | 5                         | 5               | 4               |

Significant drivers of GHG's where  $p < 0.001$  are in bold, and where  $p < 0.05$  are in bold italic font

and periods were below the global modelled average for streams (97–156 mmol m<sup>−2</sup> day<sup>−1</sup>) (Lauerwald et al. 2015). Our measurements were well below other sub-tropical and tropical forest-dominated streams (Borges et al. 2015; de Rasera et al. 2008), as well as agriculture-dominated streams, yet similar to a sub-tropical (Yao et al. 2007) and alpine stream with mixed land uses (Qu et al. 2017). Our below average flux estimates for CO<sub>2</sub> may be a reflection of the low piston velocity in sluggish waters that respond primarily to episodic flushing events (Marx et al. 2017).

CH<sub>4</sub> saturations and fluxes were highly variable temporally and spatially as often observed in inland waters (Bastviken et al. 2011). Our flux estimates (0.04 ± 0.06 mmol m<sup>−2</sup> day<sup>−1</sup>) fall within the low end of the range (4.23 ± 8.41 mmol m<sup>−2</sup> day<sup>−1</sup>) for streams and rivers in a recent global meta-analysis (Stanley et al. 2016), and are lower than agricultural and forested streams (~1.0–2.5 mmol m<sup>−2</sup> day<sup>−1</sup>) in temperate regions of Germany (Bodmer et al. 2016) and tropical and sub-tropical

streams (0.5–18 mmol m<sup>−2</sup> day<sup>−1</sup>) in Africa (Borges et al. 2015). Large discrepancies to other studies may be related to our conservative flux estimates assuming wind speeds approached zero in these sheltered waterways. N<sub>2</sub>O displayed a net-positive flux, which is comparable to that from an alpine stream on the Tibetan plateau in China (Qu et al. 2017), but higher than the forested tributaries of the Mara River in Kenya, and far lower than the modified catchments of the same river (Mwanake et al. 2019). Agricultural streams in midwestern USA, Central Kenya, and Sweden had higher fluxes of N<sub>2</sub>O (Audet et al. 2017; Beaulieu et al. 2009; Borges et al. 2015).

Calculating CO<sub>2</sub>-equivalent Sustained Global Warming Potentials (SGWP) on a 0-year timescale enables us to put in perspective the relative contribution of each GHG (Neubauer and Megonigal 2015). CO<sub>2</sub> accounted for the vast majority of the CO<sub>2</sub>-equivalent emissions (97%), despite being between 250 and 96 times less potent than N<sub>2</sub>O and CH<sub>4</sub>, respectively (Neubauer and Megonigal 2015). It is also worth noting that

**Table 5** Mean (±SD) air-atmosphere GHG fluxes and total CO<sub>2</sub> equiv. calculated from SWGPs (Neubauer and Megonigal 2015), in relation to two piston velocity models assuming 0 km h<sup>−1</sup> windspeed

| Piston velocity (k) models  | Catchment classification | Dry  |  |   | Wet  |  |   | Total CO <sub>2</sub> Equiv (20 years) g m <sup>−2</sup> day <sup>−1</sup> |
|---|--------------------------|--|--|---|--|--|---|--|
|   |                          | CO <sub>2</sub> mmol m <sup>−2</sup> day <sup>−1</sup> | CH <sub>4</sub> mmol m <sup>−2</sup> day <sup>−1</sup> | N <sub>2</sub> O μmol m <sup>−2</sup> day <sup>−1</sup> | CO <sub>2</sub> mmol m <sup>−2</sup> day <sup>−1</sup> | CH <sub>4</sub> mmol m <sup>−2</sup> day <sup>−1</sup> | N <sub>2</sub> O μmol m <sup>−2</sup> day <sup>−1</sup> |  |
| Borges et al. (2004)<br>K = 5.141u <sup>0.758</sup><br>(Sc/660) <sup>−1/2</sup>   | Agriculture              | 107 ± 35   | 0.10 ± 0.15  | 3.13 ± 2.61   | 95.5 ± 74.1  | 0.03 ± 0.05  | 5.8 ± 7.4   |  |
|   | Forest                   | 53.9 ± 28.8  | 0.02 ± 0.03  | 0.67 ± 0.32   | 101 ± 42   | 0.05 ± 0.09  | 14.5 ± 33.6   |  |
|   | Mixed modified           | 85.4 ± 43.0  | 0.04 ± 0.02  | 2.84 ± 1.91   | 76.7 ± 69.1  | 0.02 ± 0.03  | 3.34 ± 2.44   |  |
| Raymond and Cole (2001)<br>K = 1.91e <sup>0.35u</sup><br>(Sc/660) <sup>−1/2</sup> | Agriculture              | 64.1 ± 23.4  | 0.08 ± 0.16  | 2.04 ± 1.64   | 41.6 ± 33.3  | 0.01 ± 0.02  | 2.34 ± 2.32   |  |
|   | Forest                   | 67.9 ± 36.2  | 0.03 ± 0.03  | 1.09 ± 0.67   | 84.8 ± 32.5  | 0.04 ± 0.06  | 8.59 ± 17.1   |  |
|   | Mixed modified           | 72.9 ± 28.2  | 0.04 ± 0.02  | 2.91 ± 1.59   | 44.4 ± 36.8  | 0.01 ± 0.02  | 1.91 ± 1.19   |  |
| Average   | Agriculture              | 85.5 ± 26.3  | 0.09 ± 0.15  | 2.59 ± 2.05   | 68.5 ± 53.3  | 0.02 ± 0.04  | 4.07 ± 4.79   | 3.41 ± 1.84  |
|   | Forest                   | 60.9 ± 31.6  | 0.03 ± 0.03  | 0.88 ± 0.46   | 93.0 ± 33.6  | 0.05 ± 0.07  | 11.5 ± 25.2   | 3.35 ± 1.59  |
|   | Mixed modified           | 79.2 ± 34.7  | 0.04 ± 0.02  | 2.88 ± 1.67   | 60.6 ± 52.4  | 0.02 ± 0.02  | 2.62 ± 1.76   | 3.09 ± 1.97  |



CH<sub>4</sub> had a greater contribution to CO<sub>2</sub>-equivalent emissions during the dry period (1.9% dry versus 1.1% wet), while N<sub>2</sub>O had a greater contribution during the wet period (2.0% wet versus 0.8% dry) (Table 5, Fig. 9). The difference in contribution between N<sub>2</sub>O and CH<sub>4</sub> in relation to the hydrological phase highlights that hydrology can play a crucial role in driving GHGs and, accounting for this may improve current uncertainties in global models and budgets.

## Conclusions

We demonstrated that freshwater streams in sub-tropical Australia were a net source of CO<sub>2</sub>, CH<sub>4</sub>, and N<sub>2</sub>O to the atmosphere. Wet conditions drove changes in stream GHGs through the release of soil NO<sub>x</sub> and DOC following rainfall events. Groundwater discharge as traced by radon was not a major source of CO<sub>2</sub> and CH<sub>4</sub>, but seemed to influence N<sub>2</sub>O dynamics. Land use had a minor but detectable influence on dissolved greenhouse gases. CO<sub>2</sub> and CH<sub>4</sub> increased with forest area during the wet period, while N<sub>2</sub>O and CH<sub>4</sub> increased with agricultural area during the dry period. Overall, our multiple linear regression models show how DOC and NO<sub>x</sub>, rainfall events, and land use drive spatial and temporal dynamics in stream greenhouse gases in sub-tropical streams. When expressed in terms of their sustained global warming potential, the contribution of CO<sub>2</sub> emissions was about 97% while CH<sub>4</sub> and N<sub>2</sub>O combined accounted for only 3% of stream emissions. These findings have implications for improving current global outgassing estimations of GHGs in an underrepresented climatic region, and highlights the need to consider changing hydrology and land use when assessing GHG dynamics in streams.

**Supplementary Information** The online version contains supplementary material available at <https://doi.org/10.1007/s00027-021-00791-x>.

**Acknowledgements** This project was partially funded by the Australian Research Council (FT170100327; LE170100007) and the Coffs Harbour City Council Environmental Levy Grants Program. We thank Sara Lock, Stephan Conrad for running nutrient samples, and Ceylena Holloway for running DOC samples. Two anonymous reviewers and the editor provided valuable feedback that improved this manuscript.

**Authors' contributions** The paper was designed by IRS and LA. LA processed most of the data and wrote the initial drafts of the manuscript. IRS polished the text and wrote some parts of the manuscript. LFA, PDW, SAW, XC, and RE performed field and laboratory work. LCJ performed the MLR analysis. All the authors contributed to planning, data collection, data analysis, and edited the manuscript.

**Funding** Open access funding provided by University of Gothenburg. The project was funded through the Coffs Harbour City Council's Environmental Levy program and the Australian Research Council.

**Availability of data and material** The raw data used in this manuscript is available as online supplementary material.

## Compliance with ethical standards

**Conflict of interest** No conflicts of interest are associated with this paper.

**Open Access** This article is licensed under a Creative Commons Attribution 4.0 International License, which permits use, sharing, adaptation, distribution and reproduction in any medium or format, as long as you give appropriate credit to the original author(s) and the source, provide a link to the Creative Commons licence, and indicate if changes were made. The images or other third party material in this article are included in the article's Creative Commons licence, unless indicated otherwise in a credit line to the material. If material is not included in the article's Creative Commons licence and your intended use is not permitted by statutory regulation or exceeds the permitted use, you will need to obtain permission directly from the copyright holder. To view a copy of this licence, visit <http://creativecommons.org/licenses/by/4.0/>.

## References

- Atkins ML, Santos IR, Ruiz-Halpern S, Maher DT (2013) Carbon dioxide dynamics driven by groundwater discharge in a coastal floodplain creek. *J Hydrol* 493:30–42. <https://doi.org/10.1016/j.jhydrol.2013.04.008>
- Atkins ML, Santos IR, Maher DT (2016) Assessing groundwater-surface water connectivity using radon and major ions prior to coal seam gas development (Richmond River Catchment, Australia). *Appl Geochem* 73:35–48. <https://doi.org/10.1016/j.apgeochem.2016.07.012>
- Atkins ML, Santos IR, Maher DT (2017) Seasonal exports and drivers of dissolved inorganic and organic carbon, carbon dioxide, methane and δ<sup>13</sup>C signatures in a subtropical river network. *Sci Total Environ* 575:545–563. <https://doi.org/10.1016/j.scitotenv.2016.09.020>
- Audet J, Wallin MB, Kyllmar K, Andersson S, Bishop K (2017) Nitrous oxide emissions from streams in a Swedish agricultural catchment. *Agric Ecosyst Environ* 236:295–303
- Bass AM, Munksgaard NC, Leblanc M, Tweed S, Bird MI (2014) Contrasting carbon export dynamics of human impacted and pristine tropical catchments in response to a short-lived discharge event. *Hydrol Process* 28:1835–1843. <https://doi.org/10.1002/hyp.9716>
- Bastviken D, Tranvik LJ, Downing JA, Crill PM, Enrich-Prast A (2011) Freshwater methane emissions offset the continental carbon sink. *Science* 331:50. <https://doi.org/10.1126/science.1196808>
- Beaulieu J, Arango C, Tank J (2009) The effects of season and agriculture on nitrous oxide production in headwater streams. *J Environ Qual* 38:637–646
- Beaulieu JJ, Shuster WD, Rebolz JA (2010) Nitrous oxide emissions from a large, impounded river: the Ohio river. *Environ Sci Technol* 44:7527–7533. <https://doi.org/10.1021/es1016735>
- Beusen AHW, Slomp CP, Bouwman AF (2013) Global land-ocean linkage: direct inputs of nitrogen to coastal waters via submarine groundwater discharge. *Environ Res Lett* 8:034035
- Bodmer P, Heinz M, Pusch M, Singer G, Premke K (2016) Carbon dynamics and their link to dissolved organic matter quality across contrasting stream ecosystems. *Sci Total Environ* 553:574–586. <https://doi.org/10.1016/j.scitotenv.2016.02.095>
- BOM (2019) Climate statistics for Australian locations. <http://www.bom.gov.au/>

- Borges AV, Gypens N (2010) Carbonate chemistry in the coastal zone responds more strongly to eutrophication than ocean acidification. *Limnol Oceanogr* 55:346–353
- Borges AV, Vanderborcht J-P, Schiettecatte L-S, Gazeau F, Ferrón-Smith S, Delille B, Frankignoulle M (2004) Variability of the gas transfer velocity of CO<sub>2</sub> in a macrotidal estuary (the Scheldt). *Estuaries* 27:593–603
- Borges AV et al (2015) Globally significant greenhouse-gas emissions from African inland waters. *Nat Geosci* 8:637–642. <https://doi.org/10.1038/ngeo2486>
- Borges et al (2018a) Effects of agricultural land use on fluvial carbon dioxide, methane and nitrous oxide concentrations in a large European river, the Meuse (Belgium). *Sci Total Environ* 610–611:342–355. <https://doi.org/10.1016/j.scitotenv.2017.08.047>
- Borges AV, Abril G, Bouillon S (2018b) Carbon dynamics and CO<sub>2</sub> and CH<sub>4</sub> outgassing in the Mekong delta. *Biogeosciences* 15:1093–1114. <https://doi.org/10.5194/bg-15-1093-2018>
- Borges AV et al (2019) Variations in dissolved greenhouse gases (CO<sub>2</sub>, CH<sub>4</sub>, N<sub>2</sub>O) in the Congo River network overwhelmingly driven by fluvial-wetland connectivity. *Biogeosciences* 16:3801–3834. <https://doi.org/10.5194/bg-16-3801-2019>
- Burgos M, Sierra A, Ortega T, Forja JM (2015) Anthropogenic effects on greenhouse gas (CH<sub>4</sub> and N<sub>2</sub>O) emissions in the Guadaleta River Estuary (SW Spain). *Sci Total Environ* 503–504:179–189. <https://doi.org/10.1016/j.scitotenv.2014.06.038>
- Burnett WC, Kim G, Lane-Smith D (2001) A continuous monitor for assessment of <sup>222</sup>Rn in the coastal ocean. *J Radioanal Nucl Chem* 249:167–172. <https://doi.org/10.1023/A:1013217821419>
- Butman D, Raymond PA (2011) Significant efflux of carbon dioxide from streams and rivers in the United States. *Nat Geosci* 4:839–842. <https://doi.org/10.1038/ngeo1294>
- Canfield DE, Glazer AN, Falkowski PG (2010) The evolution and future of Earth's nitrogen cycle. *Science* 330:192–196
- Cole JJ et al (2007) Plumbing the global carbon cycle: integrating inland waters into the terrestrial carbon budget. *Ecosystems* 10:172–185. <https://doi.org/10.1007/s10021-006-9013-8>
- Comer-Warner SA, Goody DC, Ullah S, Glover L, Percival A, Kettridge N, Krause S (2019) Seasonal variability of sediment controls of carbon cycling in an agricultural stream. *Sci Total Environ* 688:732–741
- Conrad SR, Santos IR, Brown DR, Sanders LM, van Santen ML, Sanders CJ (2017) Mangrove sediments reveal records of development during the previous century (Coffs Creek estuary, Australia). *Mar Pollut Bull* 122:441–445. <https://doi.org/10.1016/j.marpolbul.2017.05.052>
- Conrad SR, Santos IR, White S, Sanders CJ (2019) Nutrient and trace metal fluxes into estuarine sediments linked to historical and expanding agricultural activity (Hearnes Lake, Australia). *Estuaries Coasts* 42:944–957. <https://doi.org/10.1007/s12237-019-00541-1>
- Conrad SR, Santos IR, White SA, Hessey S, Sanders CJ (2020) Elevated dissolved heavy metal discharge following rainfall downstream of intensive horticulture. *Appl Geochem* 113:104490. <https://doi.org/10.1016/j.apgeochem.2019.104490>
- Crawford JT et al (2017) Spatial heterogeneity of within-stream methane concentrations. *J Geophys Res Biogeosci* 122:1036–1048
- de Raser FFLM et al (2008) Estimating the surface area of small rivers in the southwestern Amazon and their role in CO<sub>2</sub> outgassing. *Earth Interact* 12:1–16
- Dinsmore KJ, Wallin MB, Johnson MS, Billett MF, Bishop K, Pumpunan J, Ojala A (2013) Contrasting CO<sub>2</sub> concentration discharge dynamics in headwater streams: a multi-catchment comparison. *J Geophys Res Biogeosci* 118:445–461. <https://doi.org/10.1002/jgrg.20047>
- Drake TW, Raymond PA, Spencer RGM (2018) Terrestrial carbon inputs to inland waters: a current synthesis of estimates and uncertainty. *Limnol Oceanogr Lett* 3:132–142. <https://doi.org/10.1002/lo2.10055>
- Hall RO, Ulseth AJ (2020) Gas exchange in streams and rivers WIREs. *Water* 7:e1391. <https://doi.org/10.1002/wat2.1391>
- Herreid AM, Wymore AS, Varner RK, Potter JD, McDowell WH (2020) Divergent controls on stream greenhouse gas concentrations across a land-use gradient. *Ecosystems*. <https://doi.org/10.1007/s10021-020-00584-7>
- Hope D, Palmer SM, Billett MF, Dawson JJC (2001) Carbon dioxide and methane evasion from a temperate peatland stream. *Limnol Oceanogr* 46:847–857
- Hotchkiss ER et al (2015) Sources of and processes controlling CO<sub>2</sub> emissions change with the size of streams and rivers. *Nat Geosci* 8:696–699. <https://doi.org/10.1038/ngeo2507>
- Hutchins RH, Prairie YT, del Giorgio PA (2019) Large-scale landscape drivers of CO<sub>2</sub>, CH<sub>4</sub>, DOC, and DIC in Boreal River Networks. *Global Biogeochem Cycles* 33:125–142
- Jeffrey LC, Maher DT, Santos IR, Call M, Reading MJ, Holloway C, Tait DR (2018a) The spatial and temporal drivers of pCO<sub>2</sub>, pCH<sub>4</sub> and gas transfer velocity within a subtropical estuary. *Estuarine Coast Shelf Sci* 208:83–95. <https://doi.org/10.1016/j.ecss.2018.04.022>
- Jeffrey LC, Santos IR, Tait DR, Makings U, Maher DT (2018b) Seasonal drivers of carbon dioxide dynamics in a hydrologically modified subtropical tidal river and estuary (Caboorture River, Australia). *J Geophys Res Biogeosci*. <https://doi.org/10.1029/2017JG004023>
- Jones JB Jr, Mulholland PJ (1998) Methane input and evasion in a hardwood forest stream: effects of subsurface flow from shallow and deep pathway. *Limnol Oceanogr* 43:1243–1250
- Kaine G, Giddings J (2016) Erosion control, irrigation and fertiliser management and blueberry production: grower interviews. *Coffs Harbour Landcare, Hauturu*
- Lauerwald R, Laruelle GG, Hartmann J, Ciais P, Regnier PA (2015) Spatial patterns in CO<sub>2</sub> evasion from the global river network. *Global Biogeochem Cycles* 29:534–554
- Lee J-M, Kim G (2006) A simple and rapid method for analyzing radon in coastal and ground waters using a radon-in-air monitor. *J Environ Radioact* 89:219–228. <https://doi.org/10.1016/j.jenvrad.2006.05.006>
- Li S et al (2018) Large greenhouse gases emissions from China's lakes and reservoirs. *Water Res* 147:13–24. <https://doi.org/10.1016/j.watres.2018.09.053>
- Looman A, Maher DT, Pendall E, Bass A, Santos IR (2016a) The carbon dioxide evasion cycle of an intermittent first-order stream: contrasting water–air and soil–air exchange. *Biogeochemistry* 132:87–102. <https://doi.org/10.1007/s10533-016-0289-2>
- Looman A, Santos IR, Tait DR, Webb JR, Sullivan CA, Maher DT (2016b) Carbon cycling and exports over diel and flood-recovery timescales in a subtropical rainforest headwater stream. *Sci Total Environ* 550:645–657. <https://doi.org/10.1016/j.scitotenv.2016.01.082>
- Looman A, Santos IR, Tait DR, Webb J, Holloway C, Maher DT (2019) Dissolved carbon, greenhouse gases, and δ<sup>13</sup>C dynamics in four estuaries across a land use gradient. *Aquat Sci*. <https://doi.org/10.1007/s00027-018-0617-9>
- Maavara T, Lauerwald R, Laruelle GG, Akbarzadeh Z, Bouskill NJ, Van Cappellen P, Regnier P (2019) Nitrous oxide emissions from inland waters: are IPCC estimates too high? *Global Change Biol* 25:473–488. <https://doi.org/10.1111/gcb.14504>
- MacDonald LH, Coe D (2007) Influence of headwater streams on downstream reaches in forested areas. *For Sci* 53:148–168
- Macklin PA, Maher DT, Santos IR (2014) Estuarine canal estate waters: hotspots of CO<sub>2</sub> outgassing driven by enhanced groundwater discharge? *Mar Chem* 167:82–92. <https://doi.org/10.1016/j.marchem.2014.08.002>

- Marx A et al (2017) A review of CO<sub>2</sub> and associated carbon dynamics in headwater streams: a global perspective. *Rev Geophys* 55:560–585. <https://doi.org/10.1002/2016RG000547>
- Marzadri A, Dee MM, Tonina D, Bellin A, Tank JL (2017) Role of surface and subsurface processes in scaling N<sub>2</sub>O emissions along riverine networks. *Proc Natl Acad Sci* 114:4330–4335
- Milford H (1999) Soil landscapes of the Coffs Harbour: 1: 100 000 sheet. Athol Glen Department of Land and Water Conservation, Urunga
- Musenze RS, Werner U, Grinham A, Udy J, Yuan Z (2014) Methane and nitrous oxide emissions from a subtropical estuary (the Brisbane River estuary, Australia). *Sci Total Environ* 472:719–729. <https://doi.org/10.1016/j.scitotenv.2013.11.085>
- Mwanake R, Gettel G, Aho K, Namwaya D, Masese F, Butterbach-Bahl K, Raymond P (2019) Land use, not stream order, controls N<sub>2</sub>O concentration and flux in the upper Mara River basin, Kenya. *J Geophys Res Biogeosci* 124:3491–3506
- Neubauer SC, Megonigal JP (2015) Moving beyond global warming potentials to quantify the climatic role of ecosystems. *Ecosystems* 18:1000–1013. <https://doi.org/10.1007/s10021-015-9879-4>
- Ni M, Luo J, Li S (2019) Dynamic controls on riverine pCO<sub>2</sub> and CO<sub>2</sub> outgassing in the dry-hot valley region of Southwest China. *Aquat Sci* 82:12. <https://doi.org/10.1007/s00027-019-0685-5>
- Ni M, Li S, Santos I, Zhang J, Luo J (2020) Linking riverine partial pressure of carbon dioxide to dissolved organic matter optical properties in a dry-hot valley region. *Sci Total Environ* 704:135353. <https://doi.org/10.1016/j.scitotenv.2019.135353>
- Parliamentary Counsel's Office (2013) Coffs harbour local environmental plan. NSW Government, Sydney
- Petrone KC (2010) Catchment export of carbon, nitrogen, and phosphorus across an agro-urban land use gradient Swan-Canning River system, southwestern Australia. *J Geophys Res.* <https://doi.org/10.1029/2009jg001051>
- Petrone KC, Richards JS, Grierson PF (2008) Bioavailability and composition of dissolved organic carbon and nitrogen in a near coastal catchment of south-western Australia. *Biogeochemistry* 92:27–40. <https://doi.org/10.1007/s10533-008-9238-z>
- Pierrot D et al (2009) Recommendations for autonomous underway pCO<sub>2</sub> measuring systems and data-reduction routines. *Deep Sea Res Part II Top Stud Oceanogr* 56:512–522
- Qu B, Aho KS, Li C, Kang S, Sillanpää M, Yan F, Raymond PA (2017) Greenhouse gases emissions in rivers of the Tibetan Plateau. *Sci Rep* 7:1–8
- Quick AM, Reeder WJ, Farrell TB, Tonina D, Feris KP, Benner SG (2019) Nitrous oxide from streams and rivers: a review of primary biogeochemical pathways and environmental variables. *Earth Sci Rev* 191:224–262
- Raymond P, Cole J (2001) Gas exchange in rivers and estuaries: choosing a gas transfer velocity. *Estuaries* 24:312–317
- Raymond PA et al (2012) Scaling the gas transfer velocity and hydraulic geometry in streams and small rivers. *Limnol Oceanogr Fluids Environ* 2:41–53. <https://doi.org/10.1215/21573689-1597669>
- Reading MJ et al (2020) Land use drives nitrous oxide dynamics in estuaries on regional and global scales. *Limnol Oceanogr* 65:1903–1920. <https://doi.org/10.1002/lno.11426>
- Reid ME, Iverson RM (1992) Gravity-driven groundwater flow and slope failure potential: 2. Effects of slope morphology, material properties, and hydraulic heterogeneity. *Water Resour Res* 28:939–950. <https://doi.org/10.1029/91wr02695>
- Rocher-Ros G, Sponseller RA, Lidberg W, Mörth CM, Giesler R (2019) Landscape process domains drive patterns of CO<sub>2</sub> evasion from river networks. *Limnol Oceanogr Lett* 4:87–95
- Rosamond MS, Thuss SJ, Schiff SL (2012) Dependence of riverine nitrous oxide emissions on dissolved oxygen levels. *Nat Geosci* 5:715
- Sadat-Noori M, Maher DT, Santos IR (2015) Groundwater discharge as a source of dissolved carbon and greenhouse gases in a subtropical estuary. *Estuaries Coasts* 39:639–656. <https://doi.org/10.1007/s12237-015-0042-4>
- Sawakuchi HO et al (2017) Carbon dioxide emissions along the lower Amazon River. *Front Mar Sci.* <https://doi.org/10.3389/fmars.2017.00076>
- Schade JD, Bailio J, McDowell WH (2016) Greenhouse gas flux from headwater streams in New Hampshire, USA: patterns and drivers. *Limnol Oceanogr* 61:S165–S174. <https://doi.org/10.1002/lno.10337>
- Seitzinger S et al (2010) Global river nutrient export: a scenario analysis of past and future trends. *Global Biogeochem Cycles* 24:GB0A08. <https://doi.org/10.1029/2009GB003587>
- Seitzinger SP, Kroeze C (1998) Global distribution of nitrous oxide production and N inputs in freshwater and coastal marine ecosystems. *Global Biogeochem Cycles* 12:93–113
- Smith RM, Kaushal SS (2015) Carbon cycle of an urban watershed: exports, sources, and metabolism. *Biogeochemistry* 126:173–195. <https://doi.org/10.1007/s10533-015-0151-y>
- Smith RM, Kaushal SS, Beaulieu JJ, Pennino MJ, Welty C (2017) Influence of infrastructure on water quality and greenhouse gas dynamics in urban streams. *Biogeosciences* 14:2831–2849. <https://doi.org/10.5194/bg-14-2831-2017>
- Stanley EH, Casson NJ, Christel ST, Crawford JT, Loken LC, Oliver SK (2016) The ecology of methane in streams and rivers: patterns, controls, and global significance. *Ecol Monogr* 86:146–171
- Wadnerkar PD, Santos IR, Looman A, Sanders CJ, White S, Tucker JP, Holloway C (2019) Significant nitrate attenuation in a mangrove-fringed estuary during a flood-chase experiment. *Environ Pollut* 253:1000–1008. <https://doi.org/10.1016/j.envpol.2019.06.060>
- Wadnerkar PD et al (2021) Land use and episodic rainfall as drivers of nitrogen exports in subtropical rivers: insights from δ<sup>15</sup>N–NO<sub>3</sub><sup>-</sup>, δ<sup>18</sup>O–NO<sub>3</sub><sup>-</sup> and <sup>222</sup>Rn. *Sci Total Environ* 758:143669. <https://doi.org/10.1016/j.scitotenv.2020.143669>
- Wanninkhof R (1992) Relationship between wind speed and gas exchange over the ocean. *J Geophys Res Oceans.* <https://doi.org/10.1029/92JC00188>
- Webb JR, Santos IR, Tait DR, Sippo JZ, Macdonald BCT, Robson B, Maher DT (2016) Divergent drivers of carbon dioxide and methane dynamics in an agricultural coastal floodplain: post-flood hydrological and biological drivers. *Chem Geol* 440:313–325. <https://doi.org/10.1016/j.chemgeo.2016.07.025>
- Webb JR, Santos IR, Maher DT, Finlay K (2019) The importance of aquatic carbon fluxes in net ecosystem carbon budgets: a catchment-scale review. *Ecosystems* 22:508–527
- Weiss RF, Price BA (1980) Nitrous oxide solubility in water and seawater. *Mar Chem.* [https://doi.org/10.1016/0304-4203\(80\)90024-9](https://doi.org/10.1016/0304-4203(80)90024-9)
- White SA, Santos IR, Hessey S (2018) Nitrate loads in sub-tropical headwater streams driven by intensive horticulture. *Environ Pollut* 243:1036–1046. <https://doi.org/10.1016/j.envpol.2018.08.074>
- Wilcock RJ, Sorrell BK (2007) Emissions of greenhouse gases CH<sub>4</sub> and N<sub>2</sub>O from low-gradient streams in agriculturally developed catchments. *Water Air Soil Pollut* 188:155–170. <https://doi.org/10.1007/s11270-007-9532-8>
- Yamamoto S, Alcauskas JB, Crozier TE (1976) Solubility of methane in distilled water and seawater. *J Chem Eng Data* 21:78–80. <https://doi.org/10.1021/je60068a029>
- Yao G et al (2007) Dynamics of CO<sub>2</sub> partial pressure and CO<sub>2</sub> outgassing in the lower reaches of the Xijiang River, a subtropical monsoon river in China. *Sci Total Environ* 376:255–266